UNIVERSITÀ DEGLI STUDI DI MILANO

DOCTORATE IN TRANSLATIONAL MEDICINE

FROM NUCLEUS TO MITOCHONDRIA: INSIGHTS INTO THE ROLE OF TERT IN THE PROGRESSION OF PAPILLARY THYROID CARCINOMA

Thesis of: Gabriele **POGLIAGHI**

Matr. n**. R13117**

TUTOR: Laura **FUGAZZOLA**

CO-TUTOR: Marina **MUZZA**

Academic Year 2023-2024

Table of contents

Abstract

Background:

A percentage of papillary thyroid cancers (PTCs) show higher aggressiveness and therapeutic options are limited for patients not cured by surgery and radioiodine. The reactivation of TERT is associated with poor outcome in papillary thyroid cancer (PTC). Oxidative stress (OS), caused by reactive oxygen species produced in many metabolic pathways typical of fast-dividing cells, has been identified as an important factor in cancer aggressiveness. In particular, OS could have a major impact in the progression of PTC, considering the heightened stress already suffered by the thyroid gland. Excessive levels of reactive oxygen species that can't be counterbalanced by detoxification enzymes and antioxidants can lead to apoptosis of malignant cells. Extra-telomeric functions of TERT were reported, with a protective role against OS. The aim of the present study was to explore the extra-nuclear TERT localization in PTC and its role in cancer progression.

Methods:

TERT nuclear export under OS were analysed in K1 cells, a papillary thyroid cancer cell line that recapitulates the genotype and general phenotype of the most common form of aggressive PTCs. Different plasmids have been employed: a TERT WT plasmid to study TERT localization changes, specific nuclear localized-only and mitochondrial localized-only TERT plasmids to assay increases in aggressive characteristics and metabolic changes. Proliferation, migration and glycolysis were assayed by Cell-Counting kit 8, Wound-healing assay and Glycolysis cell-based assay kit, respectively. PP2 was tested as an inhibitor of TERT export in vitro assessing the same aggressive characteristic. Thirty-nine PTCs frozen tissues were fractionated into subcellular components and tested for TERT localization, DNA damage and stress markers via Western Blot and OS by Amplex Red Reagent.

Results:

We confirmed that TERT changes its localization under OS conditions and for the first time, under treatment of the BRAF-inhibitor Vemurafenib. We discovered that TERT transfection is capable of inducing mitochondrial fragmentation, in particular when TERT localizes in extra-nuclear compartments. Moreover, we found that extra-nuclear localization of TERT is correlated with a reduction in OS levels. Mitochondrial TERT was capable of increasing proliferation, migration and glycolysis in transfected K1 cells compared to cells transfected with nuclear-limited TERT, hinting at its role in increasing aggressive capabilities of cancer cells. To exploit this new knowledge, we employed PP2, an inhibitor for the nuclear export of TERT in K1 cells and finding that it reduces proliferation, migration and glycolysis. We expanded the work by assaying whether TERT localization impacted on the phosphorylation status of key kinases. We found that mitochondrial TERT was correlated with an increase in the phosphorylation of Ser 473 of AKT. Finally, in PTC tissues the mitochondrial/nuclear ratio of TERT resulted inversely correlated with OS and p21 expression and associated with tumor persistence.

Conclusions:

Extranuclear TERT provides enhanced mitochondrial fragmentation, proliferation, migration and glycolytic potential, demonstrating its involvement in increasing the aggressive characteristics of thyroid cancer. Mitochondrial TERT in PTC tissues is associated with tumor persistence and decreased OS, confirming its involvement in reducing excess OS and thus promoting cancer cell survival. PP2 treatment can be considered effective though its action can't be reliably pinned to only its effect on the TERT export pathway.

Introduction

An introduction to Thyroid Cancer

Thyroid cancer (TC) is a common form of malignancy arising from thyroid cells and overall, the most common form of endocrine cancer. The reported incidence between males and females is around 1:3 and tends to be diagnosed at an average age of 55 years for women and 65 years for men [1].

Recently, the fifth edition of the WHO "Classification of Endocrine and Neuroendocrine Tumors reclassified the different histotypes of TC accordingly to the recent advancements in tumor biology and genetic profiles [Figure 1].

The new classification distinguished thyroid neoplasms in benign lesions, constituted by thyroid follicular nodular disease, follicular thyroid adenomas and oncocytic adenomas; low-risk neoplasms, characterised by non-invasive follicular thyroid neoplasm with papillary-like nuclear features (NIFTP), follicular thyroid tumor of uncertain malignant potential (FT-UMP), well- differentiated thyroid tumors of uncertain malignant potential (WD-UMP), hyalinizing trabecular thyroid tumors (HTT) and malignant thyroid neoplasms. The new WHO classification distinguished malignant thyroid neoplasms in follicular thyroid carcinomas (FTC), papillary thyroid carcinomas (PTC) with its several subtypes, invasive encapsulated follicular variant papillary thyroid carcinomas (IEFV-PTC), oncocytic carcinomas of the thyroid (OCA), differentiated high-grade thyroid carcinomas (DHGTC), poorly differentiated thyroid carcinomas (PDTC) and finally the rare but highly deadly anaplastic thyroid carcinomas (ATC).

FTCs are cancers usually driven by mutations in a member of the RAS family of GTPases and distinguished from PTC by lacking their nuclear cytology. Its histological subtypes are mainly classified by their tumor capsule invasive characteristics, ranging from minimally invasive to widely invasive FTCs. The follicular variant of PTC (FVPTC) is placed in the same category of FTC, as they share the same *RAS* driver mutations despite having nuclear features more closely resembling those of PTC.

OCAs, previously known as the misnamed Hurtle cell carcinomas, are classified as thyroid cancers that lack the common PTC nuclear characteristics and aggressive characteristics but present a oncocytic cytoplasm typical of dysfunctional mitochondria.

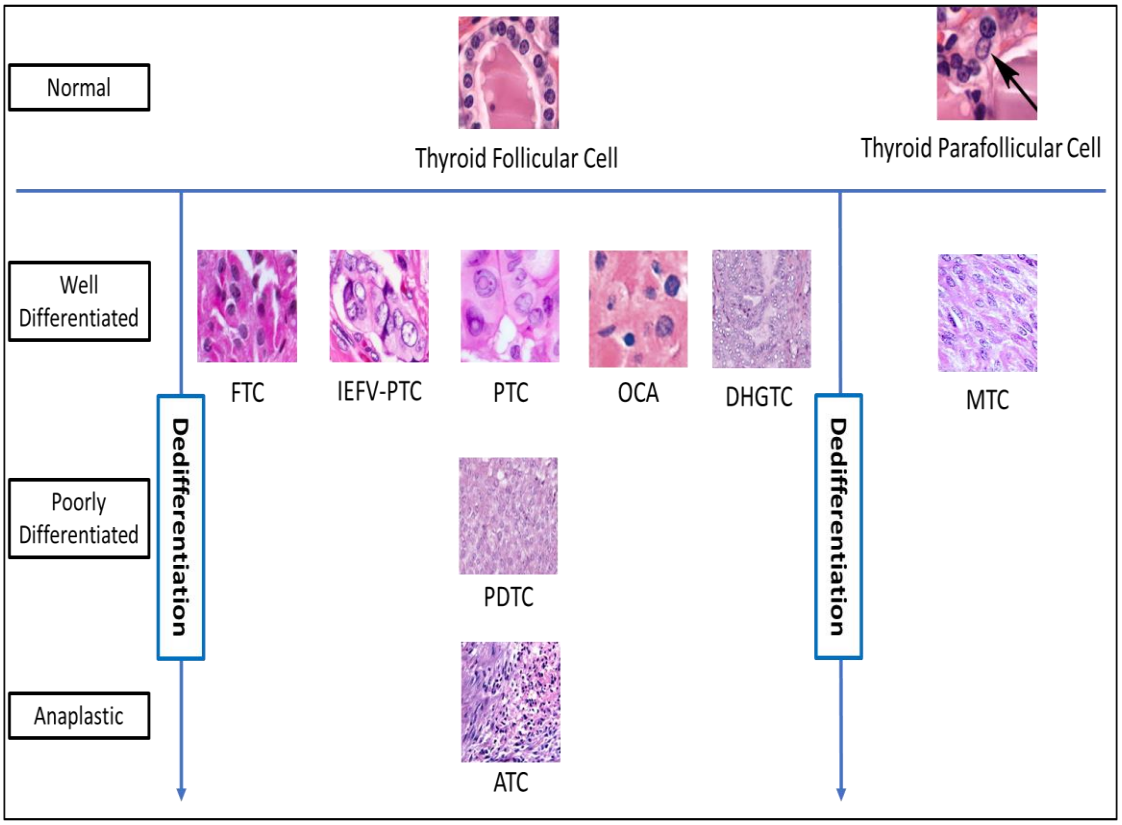

Figure 1: *Brief summarization of the new WHO 2022 thyroid cancer classification. Medullary thyroid cancers are separated from the classification due to different cell of origin. Notice the grade of dedifferentiation occurring from the well differentiated types to the anaplastic.*

Indeed, these cancers are characterized by frequent mitochondrial DNA mutations together with chromosome copy number amplifications and mutations in *EIF1AX*, *TERT*, *TP53* and *NF1*.

DHGTCs, are considered a hybrid classification between the more differentiated FTC and PTC and the more dedifferentiated and aggressive PDTC. They are characterized by presence of necrosis and ≥5 mitoses per 2 mm^2. PDTCs in contrast, are characterized by presence of necrosis, ≥5 mitoses

per 2 mm^2, lack of classical PTCs characteristics, presence of convoluted nuclei and are strongly correlated with *TERT* and *TP53* mutations.

Finally, ATCs are classified as tumors of “undifferentiated phenotype” arising by dedifferentiation of PTCs or FTCs depending on the starting driver mutation of *BRAF* or *RAS* respectively, with further presence of *TERT* promoter mutations, *TP53*, *CDKN2A* and *CDKN2B* pathogenic variants or deletions and in a subset of cases mutation in mismatch repair genes (MMR).

In contrast with all the previously mentioned variants of TC, medullary thyroid carcinomas (MTCs), arise from parafollicular cells of the thyroid and are characterized by mutations of the *RET* gene with rare cases driven by *RAS* mutations [2].

The epidemiology of thyroid cancer

Differentiated thyroid cancer (DTC) accounts for 90-95% of all TC cases, MTC for around 1-2%, PDTC for 3 to 5% and ATC for less than 1% of all cases [3].

In the last decade, a great increase in the incidence of TC has been documented worldwide with an estimated annual percentage change of 1.59 between 1990 and 2017 [Figure 2], only in part explained by overdiagnosis brought by advances in diagnostic efforts [4].

Despite this, it has been argued that lifestyle and environmental factors may impact the incidence in thyroid cancer such as Iodine and selenium intake, obesity, hormonal factors, smoking, alcohol, and chemicals such as polybrominated diphenyl ethers and organophosphate and as recently identified by our research group Perfluoroalkyl and Polyfluoroalkyl Substances (PFAS) [5,6].

General TC 5-year survival rates are excellent at 98.6% only dropping to 54.9% in cases of distant metastatic disease, 63.6% in PDTC and 12.2% in ATC [7,8,9].

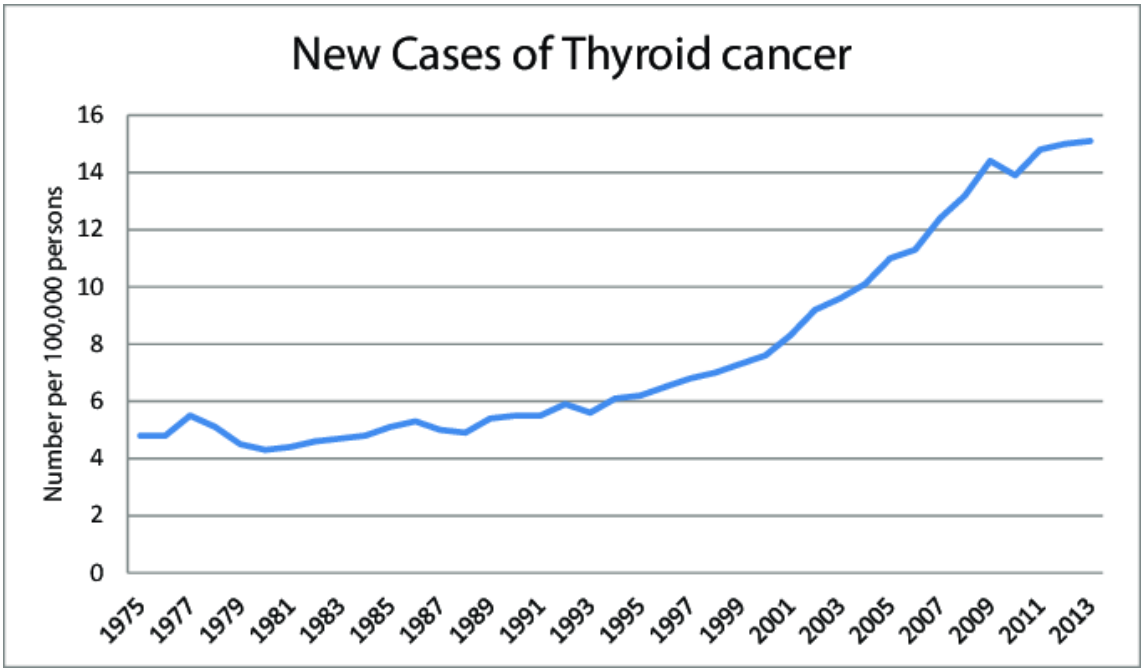

Figure 2: *Graph representing the changing incidence of thyroid cancer over the years based on the SEER cancer study (http://seer.cancer.gov/statfacts/html/thyro.html).*

Treatments options for thyroid cancer

Treatments for TC are represented by surgery, radiometabolic therapy and targeted therapy.

Surgery is usually the first suggested option for suspicious or malignant nodules. The next most important treatment option is represented by radiation therapy that in TC takes the form of radioactive-iodine treatment (RAI). Indeed, well differentiated thyroid carcinomas can still take up iodine through the NIS sodium-iodine symporter. RAI treatment is suggested as an adjuvant therapy after surgery in cases with lymphovascular invasion, distant metastases, presence of extrathyroidal extension or as a treatment for known residual cancer [11].

Targeted therapy options are suggested in cases of particularly aggressive differentiated thyroid cancers and for PDTCs and ATCs that lose their NIS expression, important for RAI therapy, due to dedifferentiation. Considering the

biology of thyroid cancer, the most important pathway for proliferation and survival is the MAPK axis and this is often targeted by multi-tyrosine kinase inhibitors (MTKIs) like lenvatinib, vandetanib and, more recently, cabozantinib. Specific targeted therapies include: dabrafenib, specific against *BRAF*, a commonly mutated gene in many TC subtypes and some cases of ATCs; selpercatinib and pralsetinib against *RET* fusions; larotrectinib and entrectinib specific for the *NTRK* gene fusions [12].

An important consideration for the use of targeted therapies is the imperative use of genetic characterization of the patient's tumor to better tailor the therapy to the individual case. Most authors suggest for this goal the employment of Next Generation Sequencing or similar high-throughput technique for the simultaneous investigation of many targetable genetic variants, a goal to which our laboratory often contributed to in recent years [13,14,15].

Papillary thyroid Cancer: from epidemiology to its many subvariants

Papillary thyroid cancer (PTC) is the most common form of thyroid malignancy representing between 80-90% of all thyroid cancers [16].

PTC is generally characterized by an excellent prognosis. It has been reported by an analysis of the American Cancer Society between 2012 and 2018 that 5-year survival rates for PTCs are at over 99.5% [17].

In contrast to the localized disease, cases with distant metastasis, that occurred in around 10% of cases, have a much reduced 5-year survival rate of 74% [18,19].

Furthermore, around two-thirds of tumors presenting distant metastases also dedifferentiate and have decreased iodine uptake, resulting in a much grimmer outcome for the patients, with a 10-year survival of between 10 and 20%. In these cases, therapeutic options are limited to tyrosine kinase inhibitors (TKI). However, TKI have important side effects and are not always associated with

a therapeutic response, but predictors of response or resistance are still unknown [19,20].

A small percentage of PTCs have a familiar occurrence (5% of familiar thyroid cancer cases) and are implicated in syndromes like the Li-Fraumeni syndrome involving *TP53* variants, Cowden syndrome implicating *PTEN*, Carney complex in cases of *PRKAR1A* mutations and finally *DICER1* syndrome involving the endoribonuclease *DICER1* responsible for miRNA maturation. In many of these cases a singular genetic cause remains unknown, being probably of polygenic origin and with variable penetrance [21,22]

The new 2022 WHO classification of papillary thyroid cancer counts nine different subvariants [Figure 3] [23]:

- Classic papillary thyroid cancer is distinguished by a still recognizable papillary growth and common presence of nuclear atypia.
- Infiltrative follicular variant distinguished by its infiltrative growth, presence of sclerosis and possible presence of multifocal foci.
- Diffuse sclerosating variant characterized by presence of psammoma bodies and chronic thyroiditis.
- Warthin-like PTCs are instead recognized by its peculiar tissue organization of papillae surrounded by oncocytic cells with a tumor core heavily infiltrated by lymphocytes.
- Solid PTCs have a solid trabecular growth behaviour with rare foci of sclerosis, lack of necrosis and high mitotic rate.
- Oncocytic PTCs are characterized by papillae lined with oncocytic cells.
- The Tall Cell variant is recognized by the presence of at least 30% of cells with height three-times the width, a “tram track appearance” of packed follicles and papillae and an eosinophilic cytoplasm.
- The columnar cell subtype has particularly shaped columnar cells with prominent pseudostratification and subnuclear vacuoles.

- The Hobnail PTC is defined by having at least 30% of cells with particularly enlarged nuclei that bulge from the apical surface, a complex papillary tissue organization with the rare presence of follicular architecture.

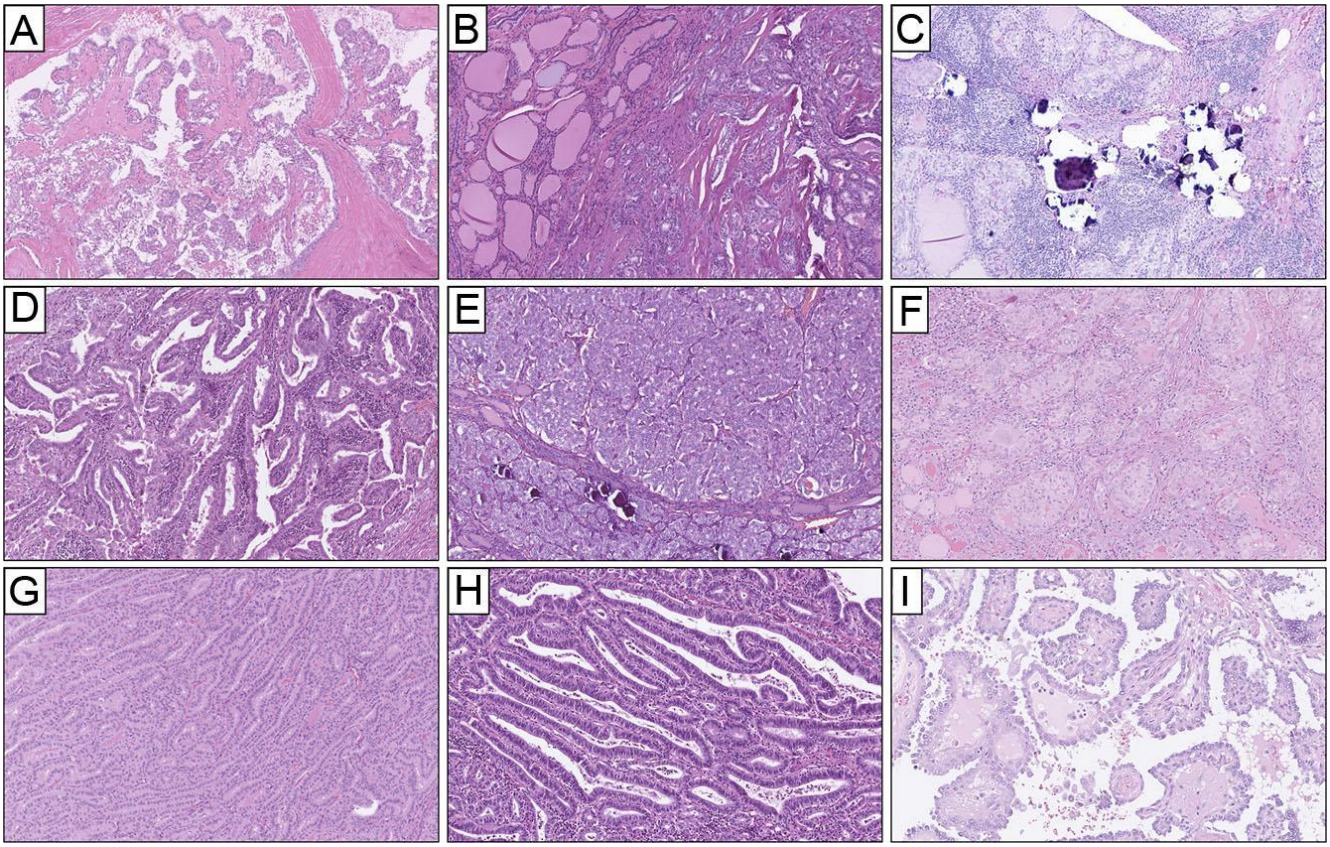

Figure 3: *Histological images representing the various PTC subtypes. A) Classical variant, B) Infiltrative Follicular variant, C) Diffuse Sclerosating variant, D) Warthin-like PTC, E) Solid PTC, F) Oncocytic PTC, G) Tall Cell PTC, H) Columnar Cell PTC, I) Hobnail PTC. Image taken from Juhlin et al. [23].*

The genetic landscape of papillary thyroid cancer

A seminal paper was published in 2014 by the Cancer Genome Atlas Network (TCGA) that helped to change the paradigm around molecular diagnosis of papillary thyroid cancer.

The TCGA group sequenced 496 PTCs and 402 normal paired tissues from U.S.A. institutes by Whole Exome Sequencing, RNA sequencing, DNA

Methylation Arrays and contributed to greatly expand the available knowledge on the genetic landscape of the disease and ultimately, to reduce PTCs without known genetic drivers to less than 3.5% of cases [Figure 4] [24].

The most common oncogene involved is *BRAF*, being mutated in 61,7% of cases. The *BRAF* gene transcribes for a member of the RAF family of serine/threonine kinases involved in the *MAPK* and *ERK* signalling pathways. The BRAF V600E mutation is the most frequent variant and is localized in the kinase domain, allowing the hyperactivation of the kinase [25].

The second most common mutations regard the RAS family of GTPases involved in the *MAPK* pathway: *HRAS*, *KRAS* and *NRAS*. The most relevant mutations amounting for 12.9% of cases fall in the codons 12,13 and 61, that are localized in the GTP binding domain and cause the constitutive activation of the protein [26].

The third most important genetic mutation regards the promoter region of *TERT*, encoding for the protein component of the telomerase. The *TERT* promoter is often mutated in a great number of tumor types such as melanoma, cancers of the central nervous system and bladder [27]. Mutations in position -124 and 146 from the start codon responsible for moderately increasing TERT expression are present in 9.4% of cases usually coexisting with the BRAF V600E mutation, which helps stratify patients with a worse outcome.

A novel gene found by the TCGA group is *EIF1AX*, responsible for around 1,5% of cases. *EIF1AX* is involved in the initiation process of protein translation and its mutations are mutually exclusive with ones involved in the *MAPK* signalling pathways.

Rarer mutations have also been reported involving gene like *PIK3CA*, *AKT1/2*, *WNT* and *PTEN*, proteins involved in the proliferation and survival pathways for the former three and a onco-suppressor for the latter.

Other important genetic events regard gene fusions, amounting to 13% of all cases and typically found mutually exclusive with other hotspot point mutations.

RET is a tyrosine kinase receptor expressed in cells of neural origin. *RET* gene fusions amount to 6,5% of all cases and all cause the rearrangement of the catalytic domain of RET with a constitutive active gene, leading to the kinase activation. The most common partner genes are represented by *CCD6*, *PRKAR1A* and *NCOA4*, also known respectively as RET/PTC 1, 2 and 3. The presence of these fusions have been reported as significantly higher in cases with a history of accidental or therapeutic radiation exposure, in children and young adults with tumors characterized by a high frequency of lymph node metastases and a classic papillary histology [28].

BRAF fusions consisting of 2.7% of cases, implicating different partner genes but still leading to an activation of the kinase domain [24].

Other fusions reported in PTC are *NTRK1*, *NTRK2* and *NTRK3* genes and *PAX8/PPARG*, amounting to 2% of cases. Similarly to RET, NTRK fusion pathogenetic mechanism rests on the constitutive activation of the tyrosine kinase domain of the *TRK* genes, activating the downstream *MAPK* and *PIK3CA* pathways. The most important fusions reported for thyroid cancer are represented by *TFG*-, *TPR*-, *TPM3* with *NTRK1* and *ETV6-NTRK3*. A recent retrospective analysis of 846 papillary thyroid cancers tissues revealed that *NTRK* fusions are mostly associated with FTC and FV-PTC thyroid cancer variants, that *NTRK3* fusions were more the prevalent form although *NTRK1* fusions were significantly correlated with higher multifocality, extrathyroidal extension, intravascular invasion and distant metastases [29].

PAX8/PPARG gene fusion, more commonly encountered in FTC and FV-PTC cases, is created by first ten exons of *PAX8* followed by either the first 8,9 or 10 exons of *PPARG*. Interestingly, the pathogenetic mechanism of this fusion is still debated, possibly working as an oncogene by suppressing the onco-

suppressive action of *PPARG* having a dominant negative effect on WT *PPARG*. Despite this, high *PPARG* expression has been detected in aggressive cases of anaplastic thyroid carcinoma [30].

Interestingly, copy number alterations were found in 27.2% of cases, mostly regarding the follicular variant of PTCs and may both represent a tumor initiating or progression specific event such as the 22q loss and 1q gain.

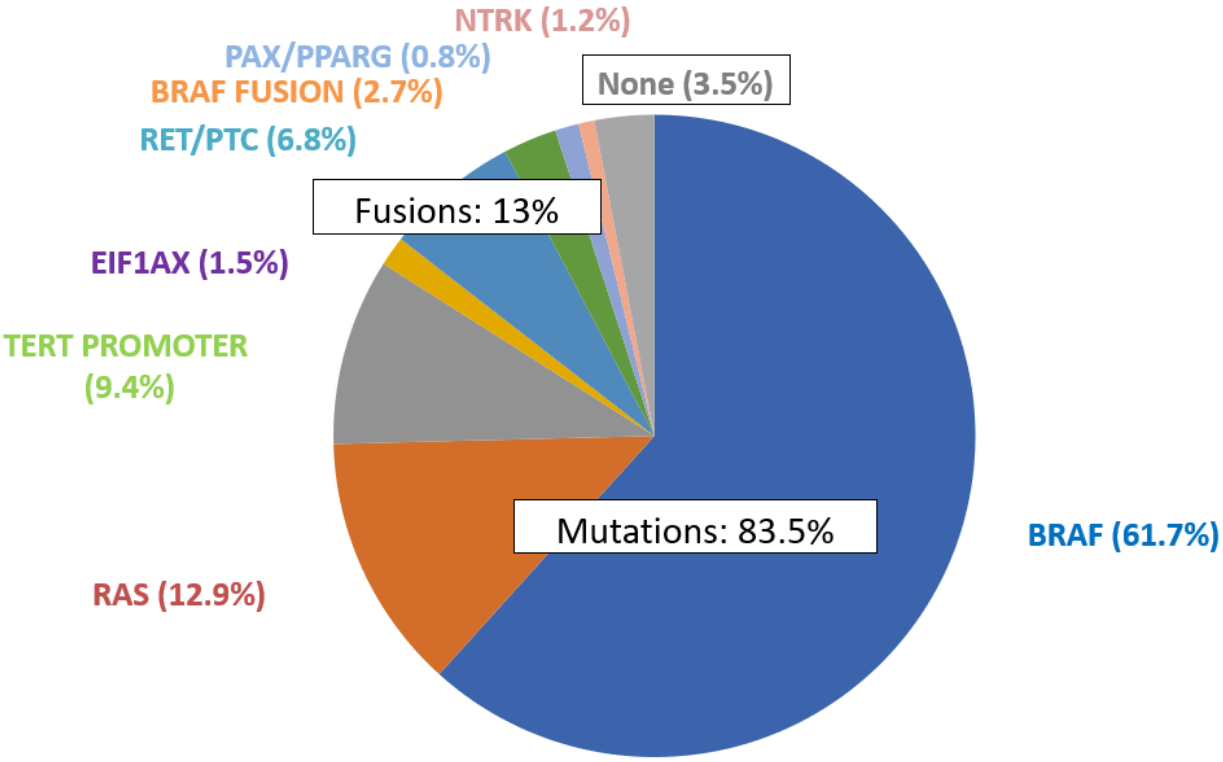

Figure 4: *Graph representing the mutational landscape of PTCs unveiled by the Cancer Genome Atlas. Most frequent mutations pertain to BRAF and RAS with a minor percentage being covered by gene fusions. 3.5% of all cases remain without a clear genetic cause.*

The TCGA group noticed that the two main mutually exclusive driver mutations of RAS and BRAF V600E had different expression of iodine uptake, metabolism and different MAPK signalling, differences that were also studied previously in mice models. The group developed a continuous (from -1 to +1) BRAF and RAS Score (BRS) and applied it to their cohort to quantify the extent of similarity

of gene expression signature from cancers with low frequency of mutations to these two extremes. As an example, the TCGA found that all *BRAF* fusions had a similar score to *BRAF* mutated PTCs and *PAX8/PPARG* fusion was similar to *RAS* mutated ones [24].

The role of Oxidative stress in cancer development and in thyroid cancer

Oxidative stress (OS) is a condition normally brought by the accumulation of Reactive Oxigen species (ROS), byproducts of cellular metabolism, taking the form of oxygen containing molecules characterized by high reactivity. ROS species can be either free radicals or nonradical molecules such as the superoxide ion O_2^- , hydroxyl radical HO^- and hydrogen peroxide (H_2O_2), respectively.

ROS are more commonly produced in mitochondria during the oxidative phosphorylation process, but other sources include cyclooxygenases and NADPH oxidases (NOXs). ROS levels are carefully managed by cells through detoxification enzymes such as superoxide dismutases, glutathione peroxidases and glutathione reductases [31].

ROS and OS have been found to have an important role in the pathogenesis of cancer. ROS can represent an important crosstalk signal between cancer cells and cancer-associated fibroblasts that can help maintain tumor homeostasis, promote invasion and proliferation. Small increases of ROS levels have also been found to activate the PI3K/AKT pathway favouring proliferation and downregulating *PTEN*, a known oncosuppressor. ROS also work by influencing epigenetic modulators such as upregulating HDACs and downregulating DNMTs [31,32].

On the other hand, excessive levels of ROS, not compensated by the antioxidant defences, can cause oxidative damage to lipids (lipid peroxidation),

proteins and DNA, leading to the death of malignant cells and thus limiting cancer progression [31].

In the normal thyroid gland, oxidative stress management is particularly important as DUOX (responsible for the calcium dependent H_2O_2 generation used for hormonogenesis) is involved in the thyroid hormone synthesis process [33]. NOX4 instead, is constitutively active in producing H_2O_2 in intracellular compartments but its role in the thyroid is, as of today, still unknown [34].

Of note, an increased expression of both DUOX and of NOX4 has been documented in PTCs tissues possibly as a signalling mechanism as suggested by the authors [35].

Research made by Azouzi and colleagues, reported a link between BRAFV600E and NOX4 expression in PTC and suggest that genes involved in thyroid differentiation might be silenced by a mechanism controlled by NOX4-derived reactive oxygen species (ROS), indicating a role of OS in the radioiodine refractoriness [36]. Our research group recently discovered that ROS generation was higher in PTCs than in the contralateral normal tissue and that OS was inversely correlated with thyroid differentiation and directly correlated with tumor stage and ATA risk in malignant tissues. GPx activity was also found increased in tumors compared with normal tissues, possibly as a compensatory mechanism against the high OS produced [37].

The Telomerase complex and its components: classical and extra canonical roles

The telomerase enzyme is responsible for the crucial maintainment of telomeres by elongation. Telomeres are structures at the end of chromosomes constituted by the repeating sequence of nucleotides $TTAGGG_n$ and by

shelterin complex proteins that bind to it, guaranteeing the chromosome stability.

The telomerase is a holoenzyme composed of a protein subunit with reverse trascriptase (RT) activity called TERT and by an RNA component that forms the template for the RT subunit called TERC. Telomerase activity has been

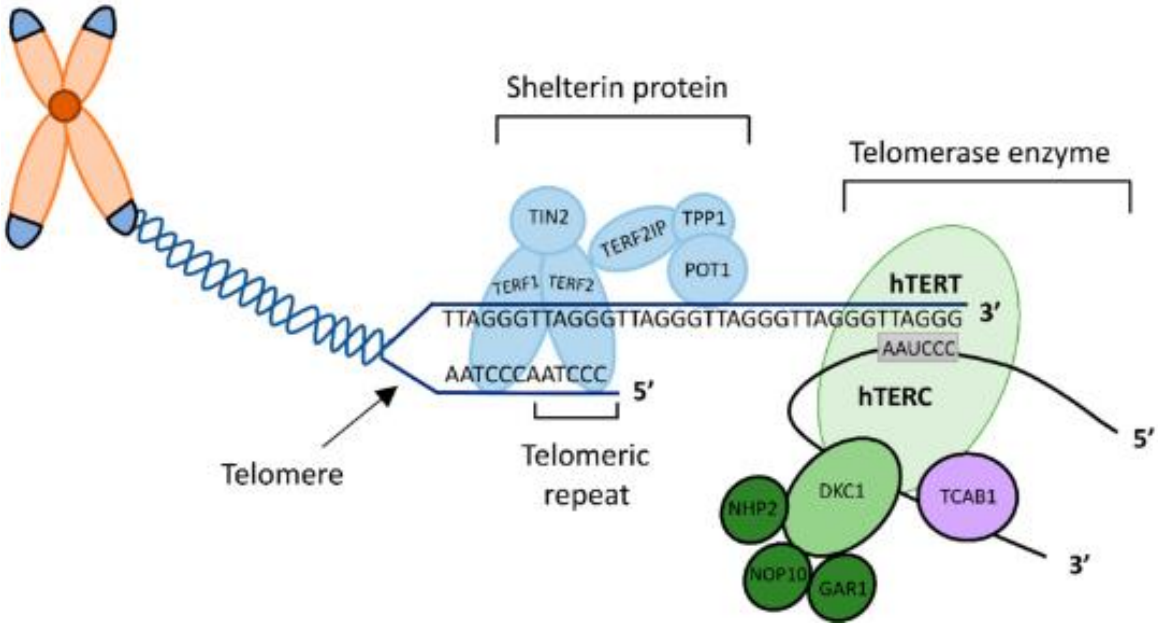

Figure 5: *The Structure of the human telomere and telomerase. Telomere is composed of tandem repeats of nucleotide sequence TTAGGG with a single stranded G-rich 3' overhang. The six-protein complex shelterin or telosome protects telomere ends. TERF1, TERF2 and POT1 directly bind to the telomere interconnected by TERF2IP, TIN2 and TPP1. Telomerase is comprised of three main components hTERT, hTERC.*

thoroughly studied over the years given its importance in the maintenance of "stemness" in stem cells and its role in immortalizing cancer cells [Figure 5] [38]. Considering its role, TERT expression levels are tightly regulated and just a few copies are normally present in non-cancerous cells. This regulation happens at many levels: through promoter methylation, miRNAs, transcription factors and alternative splicing. Methylation of the promoter region has been known as a transcription regulation mechanism. While normally hypermethylation is correlated with downregulation of a gene, in 2019 Lee and colleagues

discovered a 52 CpG island region called *TERT* Hypermethylated Oncological Region or THOR that in tumors is hypermethylated and correlated with telomerase activity and in normal tissues is demethylated. MiRNAs add another level of epigenetic regulation, in the case of *TERT* many miRNAs are found that downregulate its expression namely let-7g-3p, miR-128, miR-133a, miR-138-5p, miR-498, miR-541-3p, and miR-1182. Transcription factors that act on TERT are MYC, SP1, NF-kB, STAT3 as activators and p53, WT1, CTCF, MAD1, MAD2 and MZF-2 as transcriptional repressors. Finally, many isoforms of TERT exist beside the full-length (FL), the most important being the alpha deletion, beta deletion, and deletion of exons 4 through 13. It has been suggested that the presence of these alternative isoforms act as competitors with the expression of FL-TERT and indeed these splice variants are often expressed by normal cells [39].

Because of the ubiquitous expression in human cancers, the telomerase has been recognized as a possible therapeutic target and as a result, telomerase inhibitor drugs have garnered a lot of interest in the past ten years [40].

Besides its fundamental role in the nucleus for telomeres maintenance, recent literature demonstrated an important role for the components of telomerase in other extra-telomeric and extra-nuclear roles.

Extra-telomeric activities can be briefly summed in: gene expression regulator increasing cell proliferation, interacts with betacatenin signalling complex associating with the chromatin remodeller BRG1, by working as a RNA-polymerase producing double stranded RNA later converted by DICER1 in functional miRNAs, influencing transcription by causing histone modification by upregulating DNMT3B a methyltransferase, controlling glucose uptake by increasing the number of glucose transporters on the plasma membrane [41,42].

TERC itself has been found to have a role in preventing apoptosis, regulating DNA damage response by regulating *ATR* and activating DNA dependant protein kinases to phosphorylate hnRNP-A1. TERC RNA can work as a lncRNA

targeting *NF-kB* and increasing the release of inflammatory cytokines, but the RNA itself can be processed inside the mitochondria to produce a shorter form name TERC-53 that impairs senescence [43,44].

An important extra-nuclear role of TERT is represented by its role at the mitochondrial level by interacting with the metabolic activity of the cell by changing mitochondria copy numbers and more interestingly, its ability of managing oxidative stress [45].

TERT in the mitochondria: a factor in reducing oxidative stress

TERT has been detected in mitochondria and has been reported as a protecting factor against oxidative stress and mitochondrial DNA damage.

Haendler and colleagues proved that ROS increase, either exogenous or endogenous, was capable of causing the export from the nucleus of TERT through the nuclear pore complex via XPO1. This process is preceded by the phosphorylation of TERT in its tyrosine residue at the position 707 mediated by the Src kinase [46]. This Src-mediated effect is then terminated by Shp-2, a known regulator of the Src family, as demonstrated by Jakob et al, that found that overexpression of Shp-2 was sufficient to block the export of TERT in cells even under the stimulation of H_2O_2 [47].

Once in the cytoplasm, TERT is transported in the mitochondria thanks to its mitochondrial targeting signal (MTS) constituted by 20 amminoacids and localized at the N-terminal of the protein [48].

Different effects have been reported when the TERT protein is localized at the mitochondrial level: reduced mitochondrial DNA lesions, reduced superoxide generation, increased mitochondrial membrane potential in an anti-apoptotic function [47]. In particular, Haendler and colleagues demonstrated an interaction between TERT and Complex I of the mitochondrial respiratory chain [49], while Indran and colleagues showed that mitochondrial TERT expression was linked to higher activity of the cytochrome C oxidase [50]. Differently,

Sharma et al. suggested that TERT worked with tRNAs involved in mitochondrial DNA replication. Despite these reports, some groups suggested that the ectopic expression of TERT was instead causative on increased mitochondrial stress, higher H_2O_2 production and increased apoptosis [47]. Interestingly, mitochondrial TERT was shown to contribute to chemotherapy resistance of tumor cells by reducing ROS production and stress-induced apoptosis [38,51].

Objectives of this work

The aim of this project was to investigate whether increases of oxidative stress in the cell, operated by H_2O_2 or therapy-related, may impact the export of TERT from the nucleus to the mitochondrial compartment. Moreover, the role of mitochondrial TERT in the progression of PTCs was dissected by assessing the management of oxidative stress, proliferation, migration, metabolism and apoptosis in K1 cells in comparison to its canonical nuclear expression.

To strengthen our findings, the data obtained from the in-vitro model were then translated to frozen tumor tissue biopsies that are available at our institute and TERT localizations were correlated with clinico-pathological characteristics of the tumors.

Materials and Methods

Cell line and culture conditions

The papillary thyroid cancer derived K1 cell line (RRID: CVCL_2537) was used in these experiments. This cell line was chosen among the available papillary thyroid cancer cell lines as it most closely resembles the advanced papillary thyroid cancer genetic landscape [Table 1].

K1 Cell line (RRID:CVCL_2537)	
Disease	Papillary Thyroid Cancer
Site of origin	Metastatic site
Population	Caucasian, Italian
Doubling Time	24 hours
Sequence Variations	BRAF p.V600E; PIK3CA p.G542L; *TERT* c.1-124 C>T
TP53 Status	Wild-Type
Microsatellite Stability Status	Stable

Table 1: *K1 cell line characteristics reported from cell line databases such as "Cellosaurus" and "cancercelllines". This cell line has been selected due harbouring variants common in advanced thyroid carcinomas.*

K1 cells were grown in DMEM/F12 medium (ThermoFisher Scientific) complemented with 1% Penicillin/Streptomycin solution (Gibco) and 10% Fetal Bovine Serum (Gibco) after complement heat inactivation at 56°C for twenty minutes. Cells were kept in a humified Heracell 150i (ThermoFisher Scientific) incubator at 37°C in the presence of 5% CO2.

K1 cells were passaged routinely with Trypsin EDTA 0.25% (ThermoFisher Scientific) at a 1:4 dilution when reaching about 80-90% confluency and kept in

culture within 20 passages for all experiments to guarantee consistent experimental replicates. Cells were routinely checked for mycoplasma infection with the VenorGeM Classic (Minerva Biolabs) testing kit on DNA extracted from a reserved portion of pelleted cells used for seeding.

TERT plasmids

Three TERT plasmids [Figure 6] were employed courtesy of Professor Weinberg and Professor Jörg (University of Frankfurt).

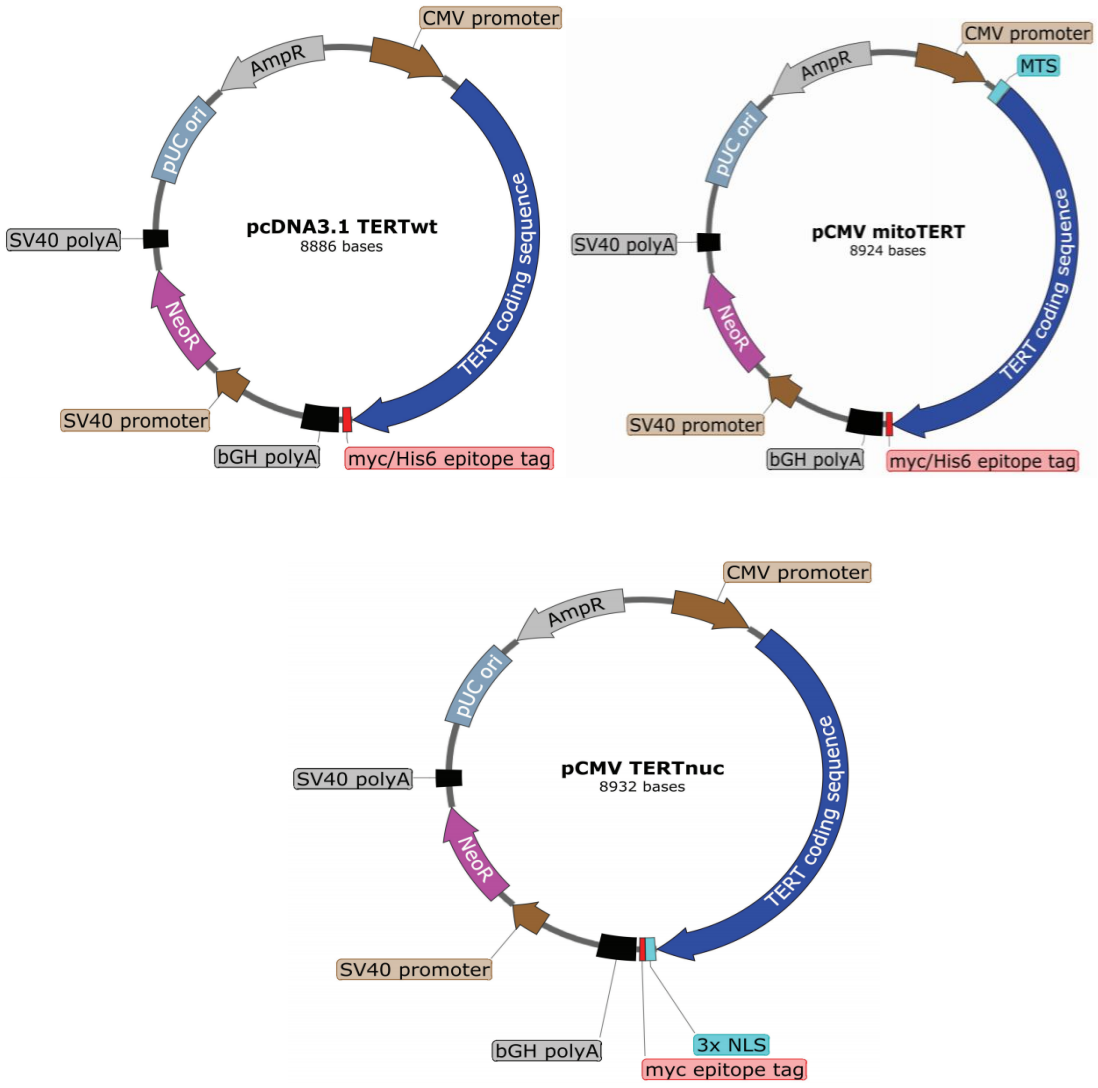

***Figure 6**: Backbone and gene insert information downloaded from "Snapgene" of TERT plasmids used in this work.*

pcDNA3.1 TERTwt carries the complete wild-type TERT coding sequence with added Myc and His tags, pCMV mitoTERT carries the complete wild-type TERT coding sequence with an added mitochondrial localization signal (MTS) added to the 5' of the transcript, a Myc and His tags, and finally pCMV nucTERT carries the complete wild-type TERT coding sequence with three nuclear localization signals added to the 3' of the transcript with a Myc tag. An empty pcDNA3.1 plasmid was also employed as a control during transfection experiments. All plasmids were quality controlled for insert sequence verification by Sanger sequencing after bacterial amplification and purification.

Evaluation of cellular oxidative stress

Ten thousand cells were counted by the Trypan Blue (ThermoFisher Scientific) method and plated in a 96-well plate (VWR). After 24 hours cells were treated in duplicate with 400 µM of H_2O_2(Med's Medical Solutions) or 10 µM of PLX4720 (MedChemExpress) for 4 hours. Cells were exposed with 5 µM H2DCFDA (ThermoFisher Scientific) following the manufacturer's protocol for 30 minutes after which fluorescence was immediately assayed with a VICTOR2 plate reader (PerkinElmer) using wavelength excitation at 485 nm and emission at 535 nm.

Immunofluorescence

Two hundred and fifty thousand cells were seeded on Matrigel (Corning) coated glass 22x22 coverslips in 6-wells plates and after 24 hours were transfected with 1200 ng of TERTwt plasmid using Fugene HD (Promega) at a 1:3 ratio, following the manufacturer's protocol. After 48 hours, cells were treated with either 400 µM of H_2O_2 or 10 µM of PLX4720 for 4 hours. To study TERT

mitochondrial localization, cells were exposed to 200nM Mitotracker reagent (Lifetech) for 30 minutes before the treatments. To inhibit TERT nuclear export, cells were pre-exposed with 10 μM of SRC inhibitor PP2 (MedChemExpress) prior the treatment with H_2O_2 for 4h. Cells were fixed with a 4% Paraformaldehyde solution in PBS and permeabilized with a 0,2% Triton X-100 solution in PBS. Cells were then exposed to 1:250 dilution of anti-Myc antibody (ThermoFisher) and 1:500 secondary antibody (Life Techno) and sealed by Vectashield Antifade with DAPI. Coverslips were then further sealed with nail polish and then visualized on a Nikon Ti Eclipse confocal microscope with the assistance of the NIS software.

The count of cells transfected with TERT wild-type plasmid was accomplished by randomly selecting at least three different fields and at least 30 cells were counted per treatment condition.

Mitochondrial dynamics investigation

The MiNA plugin [52] was downloaded from the Github website (https://github.com/StuartLab/MiNA) and installed in Fiji, a imaging processing package for ImageJ (https://imagej.net/software/fiji/). To guarantee the most replicable results, confocal images were selected on the basis of high quality of mitochondrial signal, high contrast and low crowding. Tool settings for the analysis were optimized for our experimental conditions and instrument and were applied “Median Filter”, Thresholding op “otsu”, “Use Ridge Detection” for fluorescence detection, high contrast of “100”, low contrast of “10”. Four different parameters were considered as markers for changes in the mitochondrial network: Mitochondrial Footprint, Branch Length Mean, Network Branch Mean and Summed Branch Mean. Decreased values of these four parameters were interpreted as mitochondrial fission (fragmented mitochondria) while increase values were interpreted as mitochondrial fusion [52]. Branch

Length Mean, Network Branch Mean and Summed Branch Mean were calculated and a score was derived from the median values. Score values that were <Q1 (first quartile) were interpreted as mitochondrial fission, values >Q3 (third quartile) were interpreted as mitochondrial fusion and values >Q1 and <Q3 were considered as intermediate.

Evaluation of mitochondrial oxidative stress

K1 cells were transfected with TERTwt plasmid as previously explained. After 48 hours, cells were treated with 5 μM of Mitosox reagent (Thermofisher Scientific) following the manufacturer's protocol for 30 minutes in the incubator and then fixed, prepared and analysed for immunofluorescence as previously described [53].

Cell counting assay and Glycolysis cell based assay

Ten thousand cells were seeded in 96-wells plates and after 24 hours were transfected with TERTwt, TERTmito and TERTnuc plasmids as previously described. After 48 hours from transfection, cells were treated with 400 μM of H_2O_2 or 10 μM of PLX4720 for 24 h and then 10 μl/well of Cell Counting Kit 8 (WST-8, Abcam) was added. Plates were left in the incubator for 4 hours at 37ºC and the absorbance of the medium was measured at 460nm using a Victor2 plate reader (PerkinElmer). Absorbance values were normalized to those obtained from cell transfected with an empty vector.

The level of lactate secreted into the culture medium was analysed with the Glycolysis Cell Based Assay kit (Cayman Chemicals) following the manufacture's protocol and the resulting absorbance was measured at 490nm using a Victor2 plate reader. Absorbance values were normalized to those obtained from cell transfected with an empty vector.

Wound-healing assay

Eight hundred thousand cells were seeded in 6-wells plates and after 24 hours were transfected with TERT plasmids in the previously described manner. When cells reached nearly 100% of cell confluency, the medium was changed to a fresh DMEM/F12 medium with 5% FBS concentration sufficient to limit cell stress and to avoid cell growth that may skew the analysis. A cross-shaped scratch wound was created in the monolayer using a sterile 200 µl pipette tip. Cells were then treated with fresh medium alone or supplemented with 10µM of PLX4720. Phase contrast images were captured between 0 and 8 hours using an Olympus CK2 microscope. Data are expressed as the percentages of the remaining gap area after 8 hours relative to the initial gap area. The area was measured using Fiji package of the ImageJ software. Percentages were normalized with those obtained with cells transfected with an empty vector.

Protein extraction

Cells were seeded in 6-wells plates and transfected with the TERT plasmids as previously described. 48 hours after transfection, total proteins were extracted using RIPA Buffer (ThermoFisher Scientific) with Protease Inhibitor Cocktail (Roche), following the manufacturer's recommendations. Protein extraction was enhanced by lysing cells by sonication. Protein concentration was measured by Pierce BCA assay (ThermoFisher Scientific).

Phosphorylation assessment by Proteome Profiler Human Phospho-Kinase Array Kit

Phosphorylation of 37 kinase sites involved in multiple pathways was investigated by Proteome Profiler Human Phospho-Kinase Array Kit, (R&D

Systems) [Figure 7]. Briefly, K1 cells were transfected over 48h with TERT-Mito, TERT-Nuc, TERT WT and empty vectors as previously described. Cells were lysed with a lysis buffer provided by the kit and approximately 400 ug of proteins were loaded for each gel following the manufacturer's protocol. Membranes signal was visualized with the Azure Biosystems c400 Gel Imaging System and spot densities were quantified using the Fiji package of ImageJ.

Human Phospho-Kinase Array Coordinates

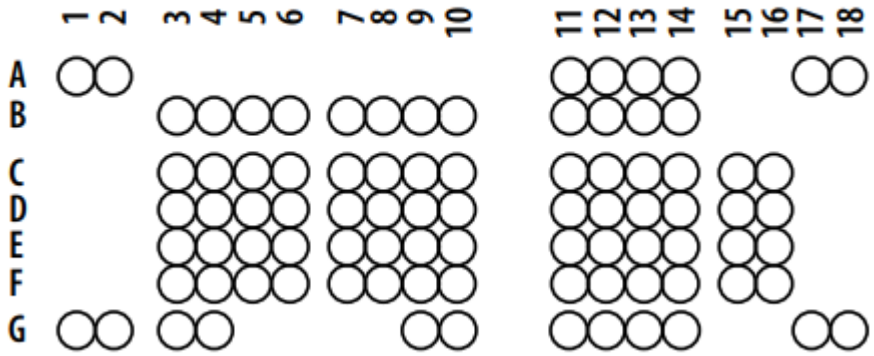

Membrane/ Coordinate	Target/Control	Phosphorylation Site
A-A1, A2	Reference Spot	——
B-A11, A12	Akt 1/2/3	T308
B-A13, A14	Akt 1/2/3	S473
B-A17, A18	Reference Spot	——
A-B3, B4	CREB	S133
A-B5, B6	EGF R	Y1086
A-B7, B8	eNOS	S1177
A-B9, B10	ERK1/2	T202/Y204, T185/Y187
B-B11, B12	Chk-2	T68
B-B13, B14	c-Jun	S63
A-C3, C4	Fgr	Y412
A-C5, C6	GSK-3α/β	S21/S9
A-C7, C8	GSK-3β	S9
A-C9, C10	HSP27	S78/S82
B-C11, C12	p53	S15
B-C13, C14	p53	S46
B-C15, C16	p53	S392
A-D3, D4	JNK 1/2/3	T183/Y185, T221/Y223
A-D5, D6	Lck	Y394
A-D7, D8	Lyn	Y397
A-D9, D10	MSK1/2	S376/S360
B-D11, D12	p70 S6 Kinase	T389
B-D13, D14	p70 S6 Kinase	T421/S424
B-D15, D16	PRAS40	T246

Membrane/ Coordinate	Target/Control	Phosphorylation Site
A-E3, E4	p38α	T180/Y182
A-E5, E6	PDGF Rβ	Y751
A-E7, E8	PLC-γ1	Y783
A-E9, E10	Src	Y419
B-E11, E12	PYK2	Y402
B-E13, E14	RSK1/2	S221/S227
B-E15, E16	RSK1/2/3	S380/S386/S377
A-F3, F4	STAT2	Y689
A-F5, F6	STAT5a/b	Y694/Y699
A-F7, F8	WNK1	T60
A-F9, F10	Yes	Y426
B-F11, F12	STAT1	Y701
B-F13, F14	STAT3	Y705
B-F15, F16	STAT3	S727
A-G1, G2	Reference Spot	——
A-G3, G4	β-Catenin	——
A-G9, G10	PBS (Negative Control)	——
B-G11, G12	STAT6	Y641
B-G13, G14	HSP60	——
B-G17, G18	PBS (Negative Control)	——

Figure 7: *Reference coordinates and detailed list of Phospho Kinases assayed on Membrane A and B of the Proteome Profiler Human Phospho-Kinase Array Kit.*

Cases

Thirty-nine PTCs were included in this work. All specimens were reviewed by a senior pathologist to confirm the diagnosis. Tumors were classified and staged according to the 8th edition of the TNM staging (AJCC) [54]. All patients were included in a thorough database which contains several clinical and pathologic information. Criteria used to identify remission or persistent/recurrent disease were drawn on the bases of the American guidelines for the management of differentiated thyroid cancer [55]. The genetic profile of tumor samples was characterized by a custom diagnostic panel performed by MALDI-TOF mass

Sample analyzed	Multiplexed PCR (Mix ID)	Mutation/ Fusion detectable
GENOMIC DNA	1	BRAF_V600E
	1	AKT1_E17K
	1	EIF1AX_c338-1GtoC
	1	NRAS_Q61R
	1	NRAS_Q61K
	1	HRAS_Q61K
	1	HRAS_Q61R
	1	TERT_G228A
	1	TERT_G250A
cDNA	2	HRAS_G13C
	2	KRAS_G12V
	2	RET_PTC1
	2	RET_PTC3
	2	TRK
	2	TRK_T1
cDNA	3	PIK3CA_E542K
	3	RET_PTC2
	3	KRAS_G13C
	3	TRK_T3

Table 2: *List of somatic point mutations and gene fusions targeted by the PTC-MA panel and genetic material used for the analysis.*

spectrometry Sequenom (Sequenom, Agena) called PTC-MA panel, capable of detecting at the same time 13 of the most common hotspot mutations and 6 frequent fusion genes reported in thyroid cancer, as was previously reported by our group [14] [Table 2].

The study was approved by the Ethical Committee of the Institution involved (CE 2020_12_15_03).

Tissue fractioning and collection of subcellular components

Surgery samples were cut to remove fibrous tissue and homogenized using a Dounce homogenizer in 50 mM sodium phosphate buffer (pH 7.2) containing 0.25 M sucrose, 0.5 mM dithiothreitol, 1 mM EGTA and protease inhibitors (Roche). Homogenates were filtered, centrifuged at 500 g at 4°C to remove intact cells which we considered the total fraction. The supernatant was centrifuged at 630g for 10 min to isolate the nuclear fraction. The supernatant was then centrifuged at 10000g for 20 min to isolate the mitochondrial and cytoplasmic fractions. Protein concentration was measured by Pierce BCA assay (ThermoFisher Scientific).

Western blot analysis

Thirty µg of total proteins from cell or tissues were resolved by electrophoresis on a gradient 6-12% SDS-PAGE under reducing conditions and immunoblotted with anti-PARP, P21 and γH2AX antibodies (Cell Signaling). Nuclear and mitochondrial fractions from tissues were resolved by electrophoresis and immunoblotted anti-TERT (Rockland) and P85 (Thermofisher) or VDAC (Santa

Cruz) antibodies, respectively. As a reference, total proteins were extracted from K1 cells in RIPA buffer (Thermo Fisher Scientific) and 30 µg were loaded in each Western blot experiment together with the tissue fractions. Membranes after transfer were exposed to 1:1000 dilution in 5% milk of primary antibodies overnight followed by a 1:5000 dilution of HRP-conjugated secondary antibodies. Membranes were then exposed to WESTAR Supernova HRP detection substrate and the signal visualized by Azure Biosystem c400 Imager (Azure Biosystems). Cleaved and total PARP, P21 and γH2AX signals were normalized to β-actin signals. TERT signals in nuclear or mitochondrial fractions were normalized to P85 or VDAC signals, respectively. Normalized band intensities of the samples were divided for that obtained in the loading control.

Measurement of oxidative stress in PTC tissues

OS was evaluated by measuring ROS production in the cytoplasmic fraction of the tumors, as our group recently reported [37]. In particular, 20 µg of cytoplasmic fraction were incubated in 150 mM sodium phosphate buffer (pH 7.4) containing 1 mM EGTA, 100 U/mL superoxide dismutase (SOD), 0.5 U/mL horseradish peroxidase (Merck) and 50 mM Amplex Red Reagent (Invitrogen), and the fluorescence was measured in a Victor2 plate reader (PerkinElmer) at 37°C, using wavelength excitation at 535 nm and emission at 610 nm. H_2O_2 production was quantified using standard calibration curves and specific activity was expressed as nmol per milligram of protein per hour. Each sample was analysed at least in two independent experiments and results are expressed as average.

Statistical analyses

Experiments were always performed at least in triplicate. Statistical analyses were performed with Graphpad software. T-student (or Wilcoxon test), Chi-square (or Fisher' exact test), Pearson correlation (or Spearman non-parametric correlation), One-way ANOVA and Two-way ANOVA tests were employed depending on the normality distribution of the variables assayed. Statistical analyses were also reviewed by a biostatistician.

Results

Quantification of stress levels change in K1 cells under stress conditions

We began by verifying the generated OS levels in K1 cells in response to treatment with 400 µM of H_2O_2 or with 10 µM of PLX4720 for 4 hours. Cells showed an expected increase of intracellular OS in response to H_2O_2 and a lesser one with PLX4720 treatment (P=0.004 and 0.008; n=3) [Figure 8].

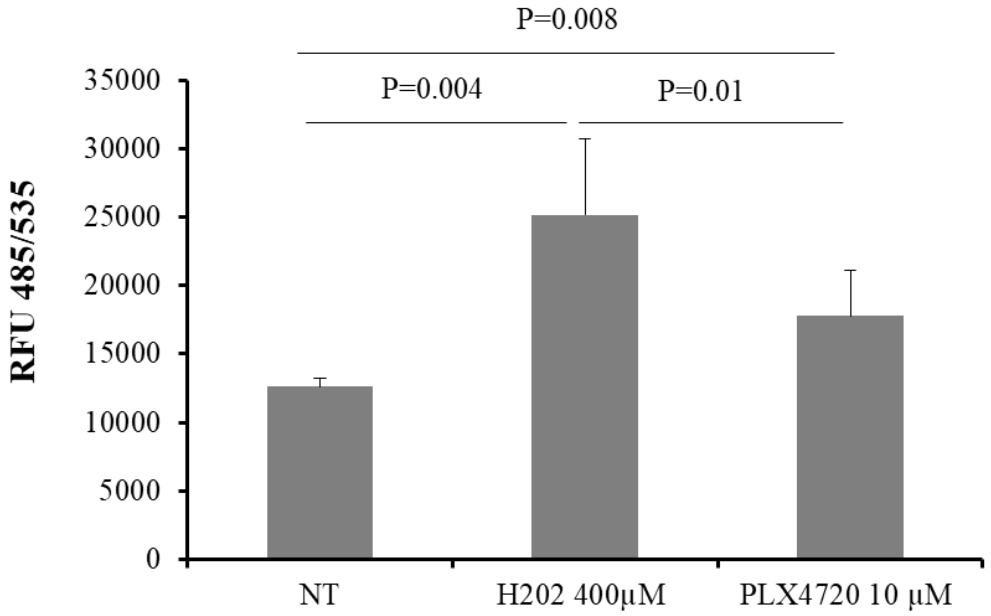

Figure 8: *Graph representing the oxidative stress generated by K1 cells in response to treatment with 400 µM of H_2O_2 or 10 µM of PLX4720 after 4 hours, measured in relative fluorescence units (n=3).*

TERT wt localization pattern in normal and stress conditions

TERT wild-type localization was assayed by confocal microscopy. Nucleus were marked with DAPI staining and TERT localization is marked by Alexa Fluor 488- conjugated secondary antibody. To mark mitochondria in our cells, we used the MitoTracker Orange CMTROS fluorescent marker. In accordance with

the literature and its role in telomere maintenance, TERT protein in untreated conditions was mostly detected in the nucleus. The immunofluorescence experiment showed a change in localization of the TERT protein to the cytoplasm in response to an oxidative stress challenge in the form of 400 µM of H_2O_2 or 10 µM of PLX4720, with a partial co-localization of TERT with the mitochondria signal (yellow co-localization signal) [Figure 9].

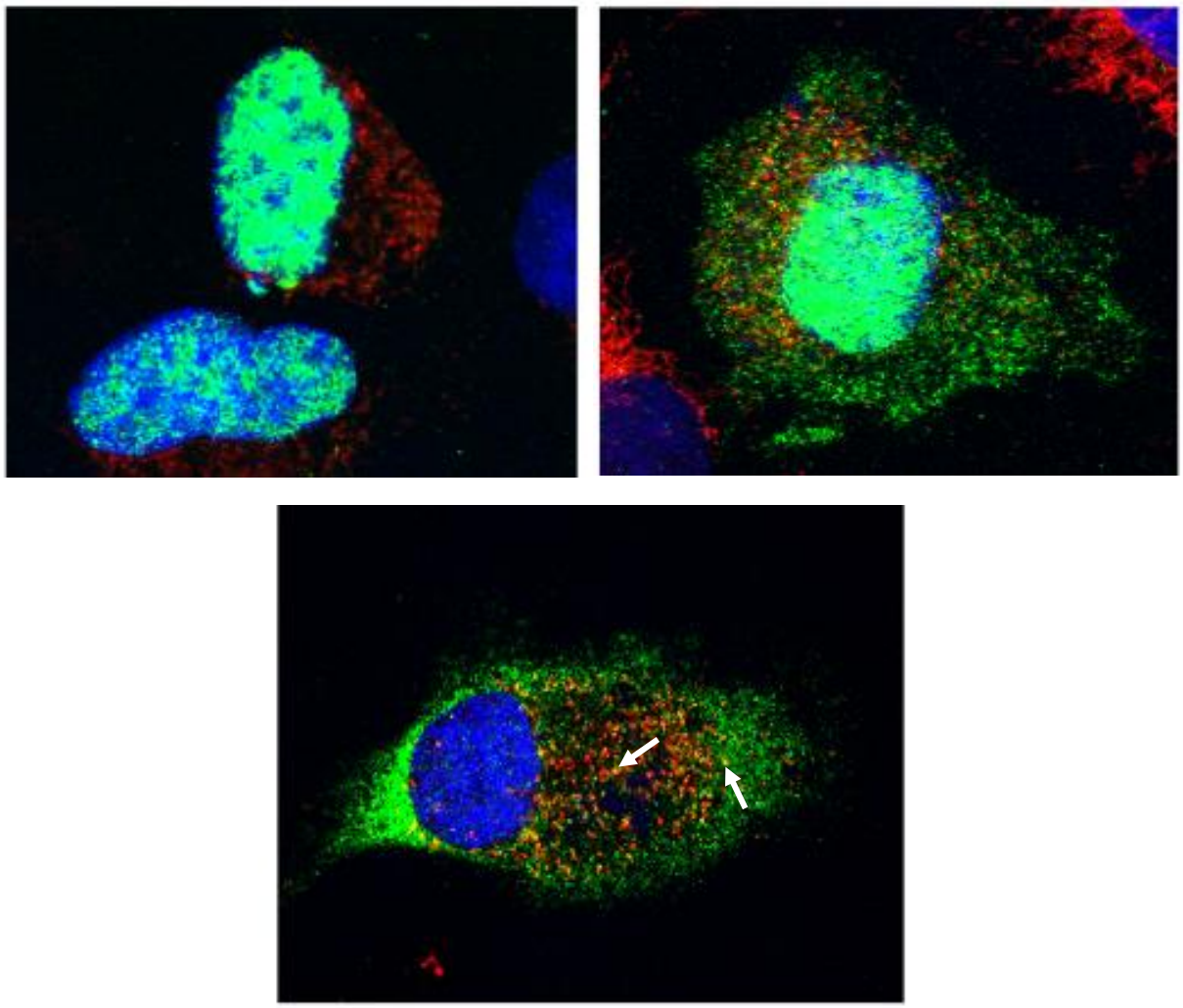

Figure 9: *Different patterns of TERT expression in K1 cell line transfected with Tertwt plasmid in untreated conditions (A) and under oxidative stress conditions (B,C). Partial colocalization signal marked by the yellow merging signal (white arrows in panel C) (blue: DAPI, green: hTERT, orange: Mitotracker, 60x magnification).*

Quantification of TERT localization change in K1 cells under stress conditions

Considering the change of localization, we wanted to assess and quantify the extent to which oxidative stress impacted the rate of extra-nuclear TERT in K1 cells transfected with the TERT wt plasmid. Cells were assessed after 4 hours in untreated, challenged with H_2O_2 and PLX 4720 as previously detailed.

We found an increase in the number of cells with extra-nuclear TERT signal in both H_2O_2 and PLX4720 treatment ($P<0.0001$ and 0.01, respectively; n=4). Interestingly, while TERT nuclear export was reported in the literature in fibroblasts after treatment with H_2O_2, to the best of our abilities it is the first time that a similar behaviour has been obtained with cells treated with PLX4720 [Figure 10].

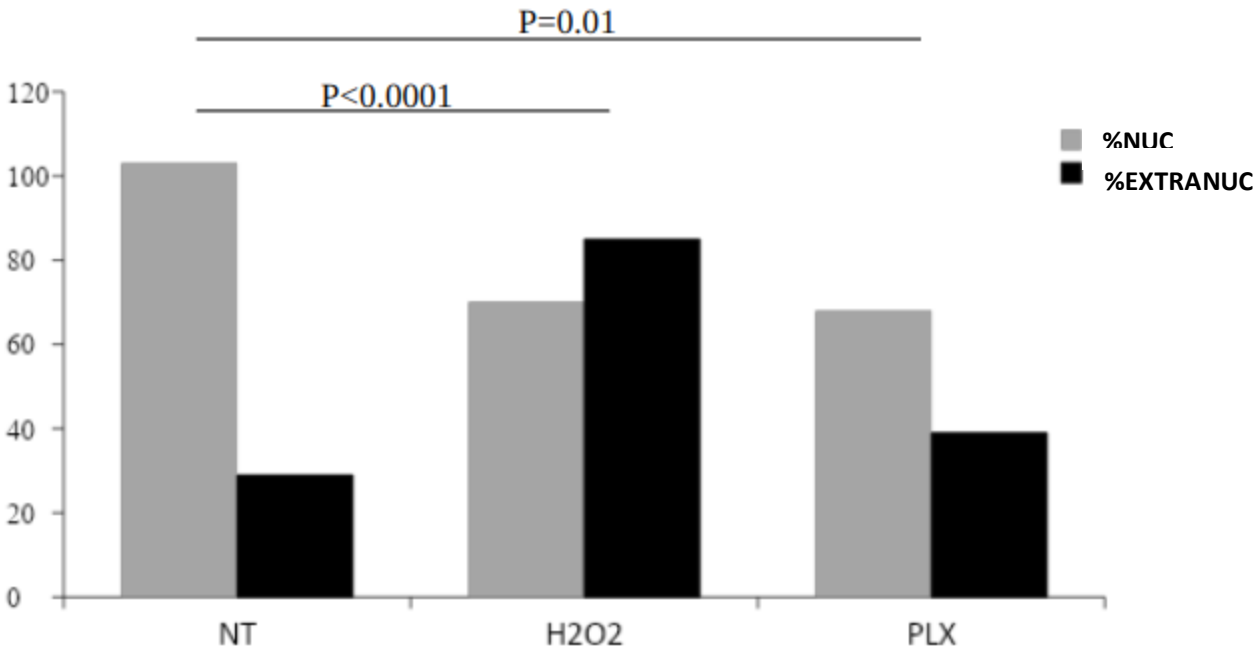

Figure 10: *Graph representing the manual count of cells with a specific nuclear or extranuclear pattern in untreated (NT), H_2O_2 and PLX4720 (PLX) treated conditions. The bars height corresponds to the number of cells with the specific characteristic (n=4).*

Mitochondrial Dynamics investigation with MiNA plugin

During our localization experiments with the transfected TERT wt plasmid, we noticed that mitochondria in transfected cells had a considerably smaller size and were “punctiform” in appearance. As in the literature it was recently reported a role of TERT into the maturation of PINK1, an important factor for mitophagy, we decided to perform an analysis on the mitochondrial dynamics considering a possible role for TERT [54].

For this purpose, the MiNA plugin for Fiji was employed as it allows for the analysis of mitochondrial dynamics using images from confocal immunofluorescence.

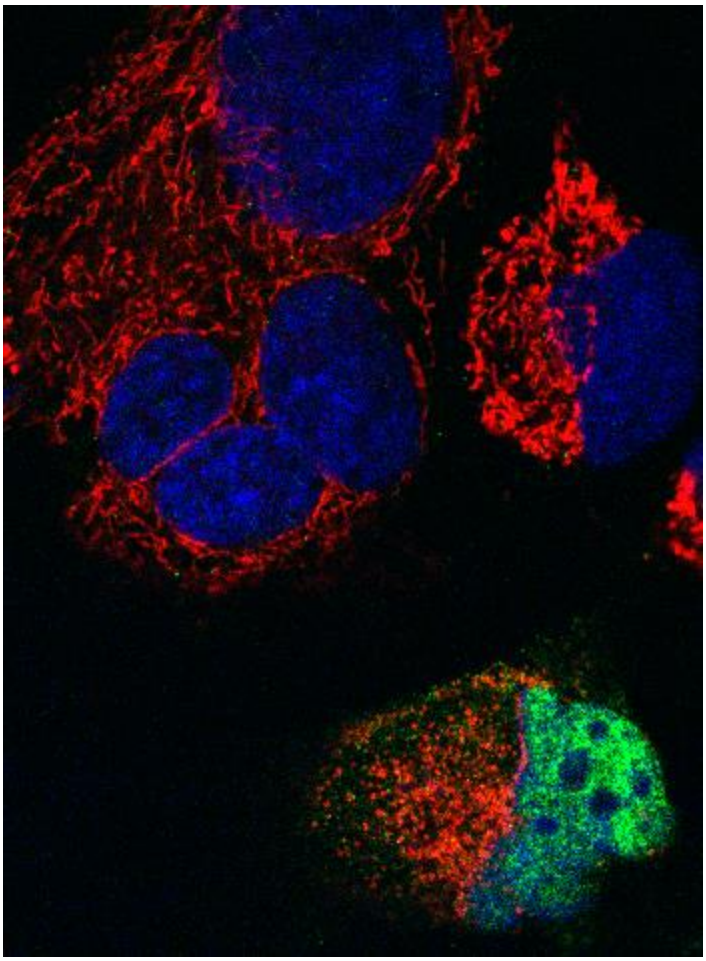

Figure 11: *Representative image of TERT wt transfected K1 cells under H_2O_2 treatment conditions, highlighted is the different mitochondrial pattern between untransfected cells and cells with mixed nuclear and cytoplasmic signal (blue: DAPI, green: hTERT, orange: Mitotracker, 60x magnification).*

The pictures collected for the previous experiment were further selected for those of highest quality and signal contrast and were then processed with the MiNA plugin as described in the Materials and Methods section.

Firstly, we found that in response to OS mediated by H_2O_2, cells transfected with the empty vector displayed higher mitochondrial fission compared to untreated conditions (P=0.0002) and to cells treated with PLX4720 (P<0.0001) [Figure 11].

We then studied whether TERT transfection and its different localization could be associated with changes in the mitochondrial network.

Cells transfected with the TERT WT vector demonstrated an increase of mitochondrial fission with either TERT located to the nucleus or to the cytoplasm compared to untransfected cells (P=0.002 and P<0.0001, respectively; n=4), although cells presenting an extra-nuclear localization pattern of TERT displayed a higher mitochondrial fragmentation than nuclear TERT (P=0.01; n=4).

Extra-nuclear TERT localization in K1 cells treated with H_2O_2 resulted in a higher mitochondrial fission compared to both nuclear TERT (P=0.01; n=4) and untrasfected cells (P=0.0002; n=4).

Interestingly, in PLX4720 (vemurafenib) treated cells, both nuclear and extra-nuclear TERT were able to induce a higher mitochondrial fission compared to untrasfected cells (P<0.0001; n=4), but the level of mitochondrial fragmentation was higher in extra-nuclear than in nuclear localization (P=0.0006; n=4) [Figure 12].

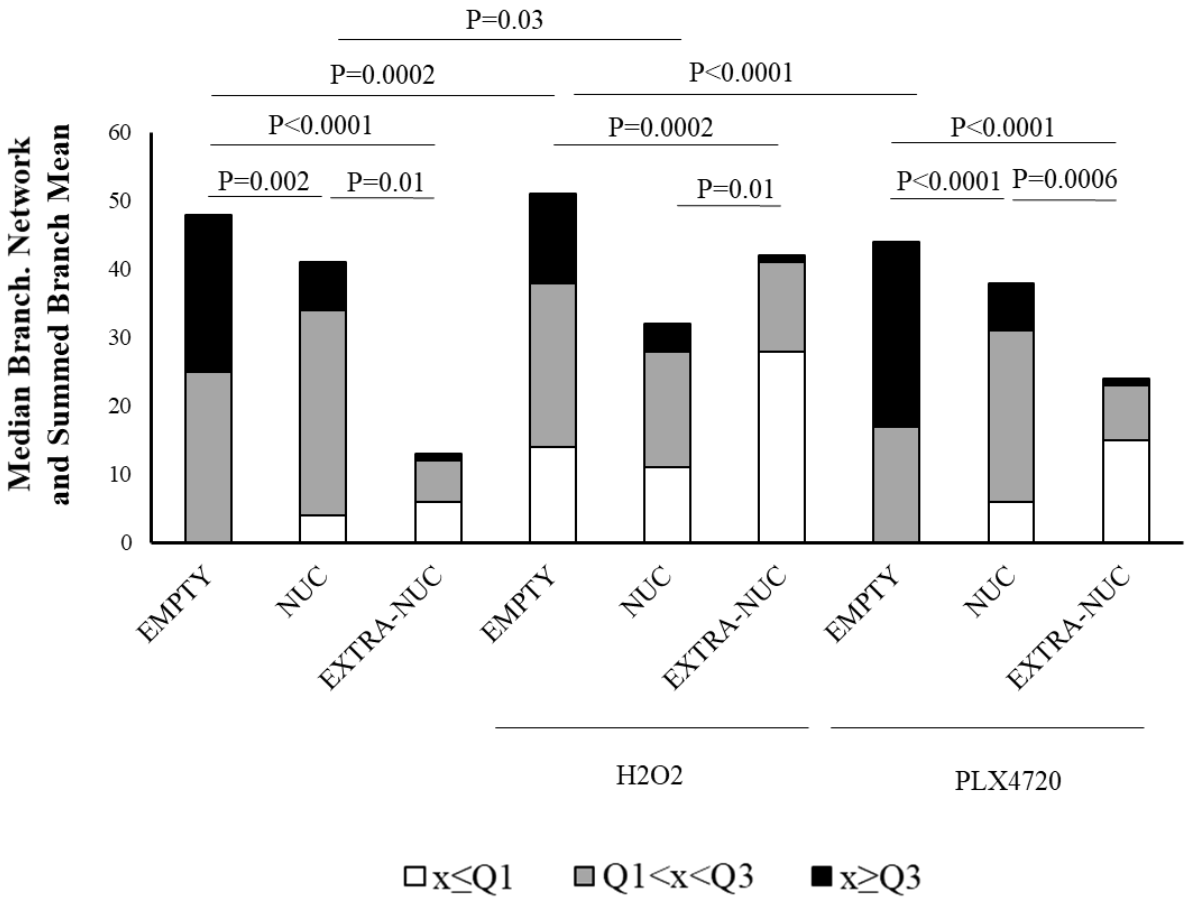

Figure 12: *Bar graph representing the change in mitochondrial dynamics in K1 cells transfected with TERT wt based on TERT localization in untreated, H_2O_2 or PLX4720 treated conditions. EMPTY: empty vector, NUC: nuclear TERT localization, EXTRA-NUC: extra-nuclear TERT localization, Q1: first quartile; Q3: third quartile (n=4).*

Mitochondrial Stress investigation with Mitosox in transfected cells

To study whether TERT transfection and its different sub-cellular localization affected the amount of mitochondrial OS produced, we transfected K1 cells with TERT WT plasmid and an empty plasmid. Cells were then exposed to Mitosox reagent to detect mitochondrial-derived oxidative stress in basal conditions or treated with H_2O_2.

After treatment with H_2O_2, cells transfected with the empty vector had a

significant increase in mitochondrial produces OS compared to untreated cells (P=0.04; n=3). This increase was not observed in cells overexpressing TERTwt. Indeed, K1 cells overexpressing TERT WT both localized in the nucleus or in the extra-nuclear compartment showed a significant decrease in mitochondrial OS produced after H_2O_2 treatment in comparison with cells transfected with the empty vector (P=0.02 and 0.01, respectively; n=3).

Interestingly, the extra-nuclear TERT localization was capable of inducing a higher reduction of mitochondrial OS compared to the nuclear TERT localization, in H_2O_2 treated cells (P=0.04; n=3) [Figure 13].

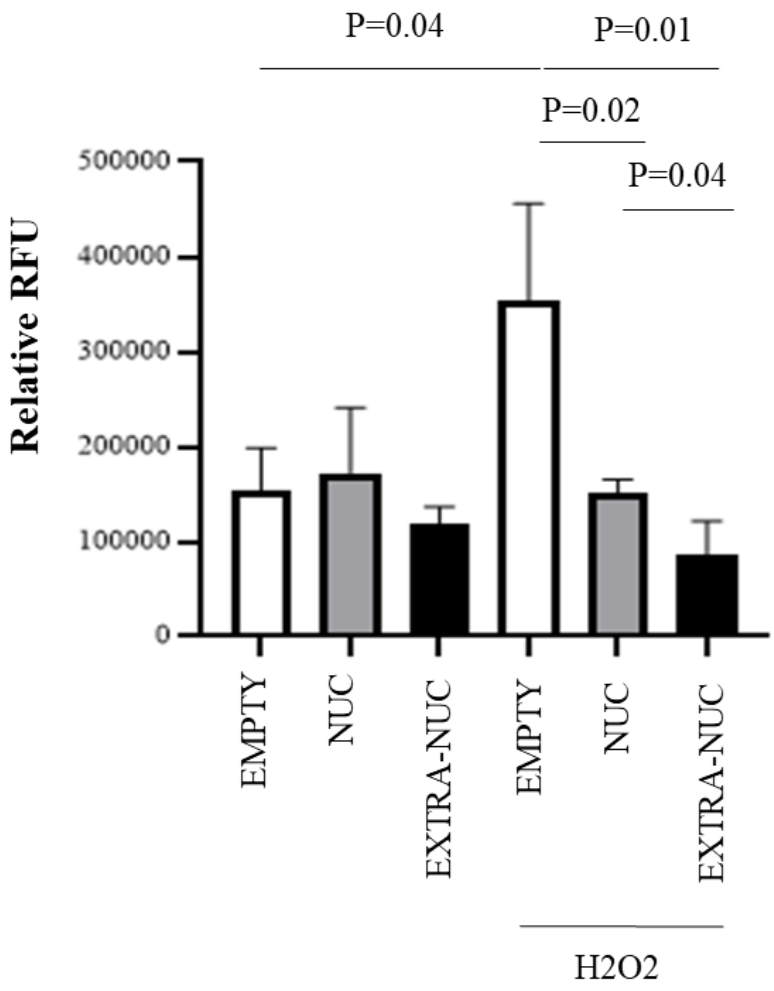

Figure 13: *Bar Graph representing the impact of Oxidative stress assayed by MITOSOX reagent on K1 cells transfected with TERT WT and empty plasmids (n=3).*

Cell proliferation assay

To assess whether limiting TERT localization has an effect on the proliferation ability of cells, K1 cells were transfected with nuclear localization limited (nucTERT) or mitochondrial localization limited (mitoTERT) specific constructs. Cells were then analyzed by the CCK-8 kit capable of assessing proliferation in a highly sensible manner without damaging the cells and by-passing the usual mitochondrial of assay with tetrazolium salts, that could be skewed by anomalous mitochondrial activity, such as mitochondrial fission, using instead cytoplasmic enzymes [55]. We found that cells transfected with mitoTERT showed higher proliferation rate than those transfected with nucTERT (P=0.02; n=6) [Figure 14].

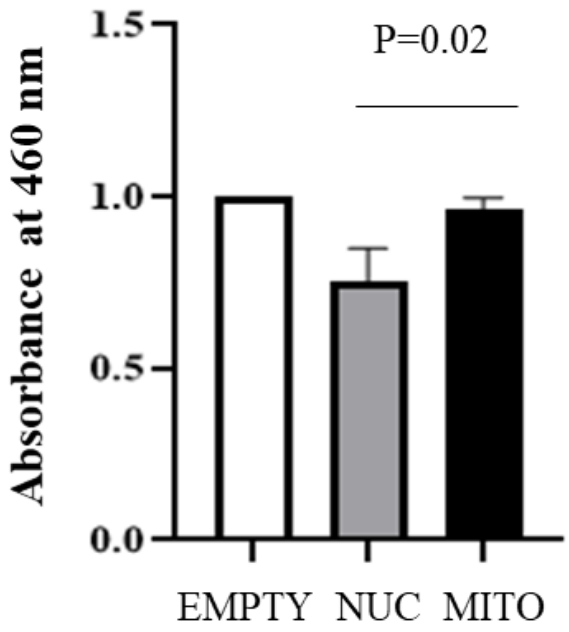

Figure 14: *Graph of absorbance data normalized on the empty vector. TERT WT-transfected cells had increased proliferation compared to localization-limited TERT plasmids (n=6).*

Glycolysis assay

Considering the link reported in the literature between mitochondrial

fragmentation and glycolytic metabolism [56], we decided to test the possibility that TERT localization might have an impact on glycolysis. We discovered that cells transfected with mitoTERT had an increased lactate production (lactate being the end product of the glycolytic process) than cells transfected with nucTERT (P= 0.002; n=6) [Figure 15].

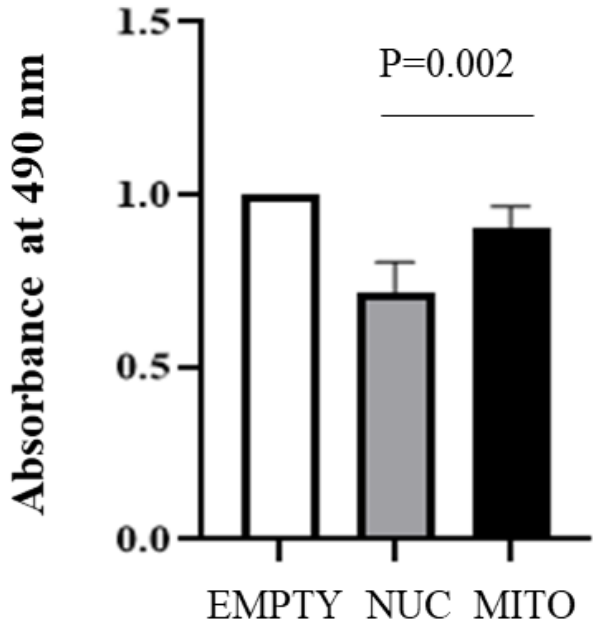

Figure 15: *Absorbance data normalized on the empty vector. TERT mito had an increase in glycolytic potential than TERT localized in the nucleus (n=6).*

Wound-healing assay

To complement our proliferation assay, we decided to assess whether different TERT localizations might impact on K1 cells' migration abilities by performing the wound-healing assay. Interestingly, we found that cells transfected with mitoTERT plasmid had increased migration capabilities than those transfected with the nucTERT plasmid (P=0.04; n=5) [Figure 16].

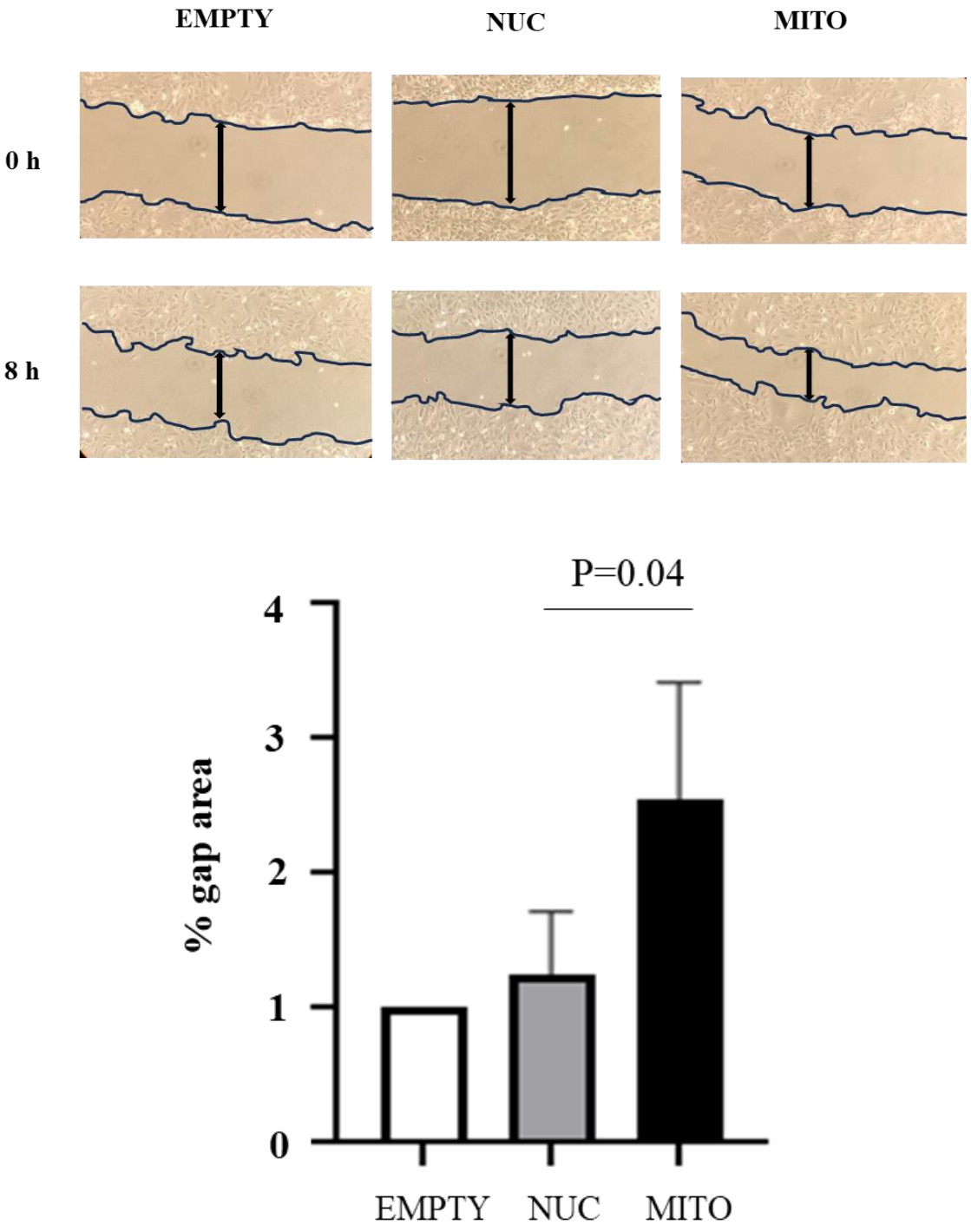

Figure 16: *(Above) Representative inverted microscope images of wound healing assays on K1 cells transfected with nucTERT, mitoTERT or an empty plasmid used as a control. (Below) Graph representing the gap area closed over 8 h compared against the empty plasmid (n=5).*

PP2 effect on K1 cell line

To get more insights into the results obtained at the nuclear level, we treated cells with 10 µM of PP2, a SRC kinase inhibitor, that is responsible for the start of TERT nuclear export process [42]. According to the data obtained with the nucTERT plasmid, treatment with PP2 significantly reduced K1 proliferation, lactate generation (P=0.01 and 0.03, respectively; n=3) and migration compared to mock-treated cells (P=0.002; n=3) [Figure 17].

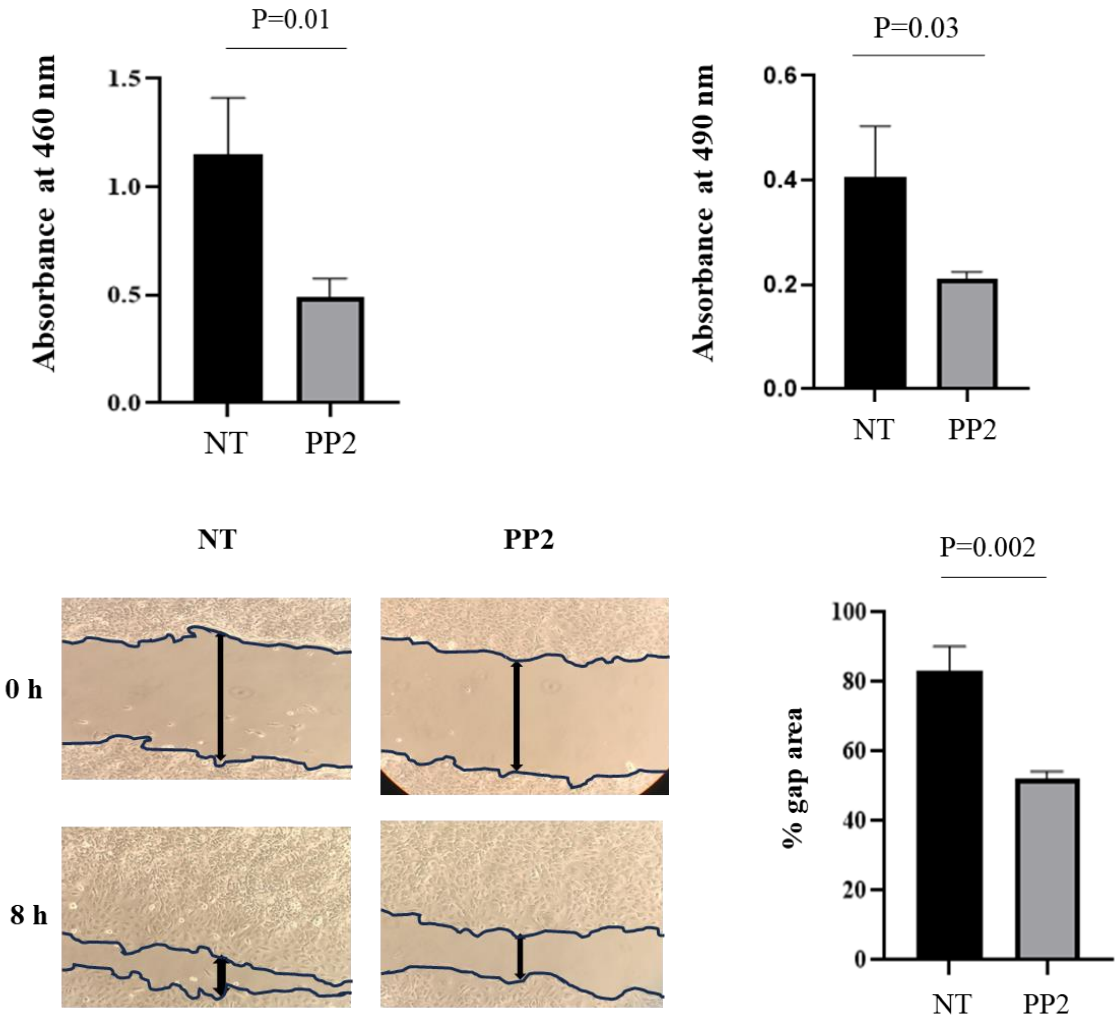

Figure 17: *(Top Left) Absorbance levels in cells treated with PP2 and control, proliferation; (Top Right) graph representing the absorbance levels corresponding to glycolysis level in cells treated with PP2 and control (Bottom Left) representative images of wound-healing assay of K1 cells untreated and treated with PP2 (Bottom Right) graph representing the percentage of reduction of gap area in cells treated with PP2 and control.*

TERT localization and effect of phosphorylation assay

We found that TERT localization had an effect in the proliferation, migration, and lactate production. As phosphorylation is an important post-translational modification implicated in many cellular processes and different signal cascades, we decided to test if TERT localization (using the specific nucTERT and mitoTERT plasmids) had an impact on the phosphorylation of the most classical signaling pathways with the Human Phospho-kinase Array kit (see Materials and Methods and Figure 7 for a list of targets and transfection information). Of the 37 kinases investigated, the phosphorylation of AKT Ser473 showed the highest difference between mitoTERT and nucTERT, around 2.4 folds (n=1) [Figure 18,19].

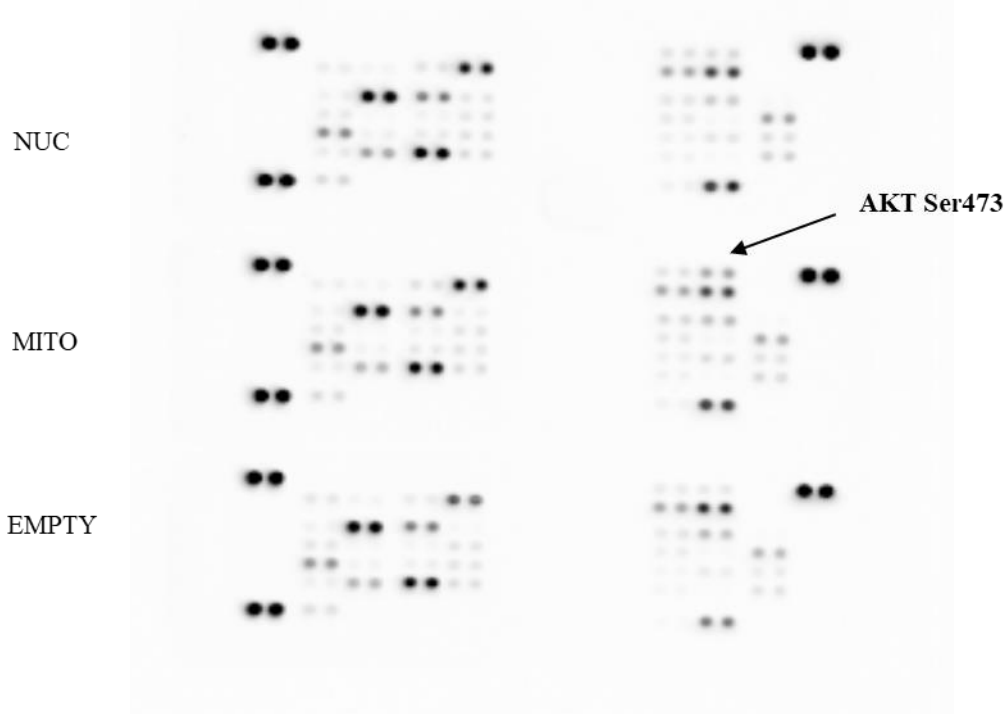

Figure 18: *Signals obtained from membrane A and B of the Proteome assay visualized with the Azure imaging system with the recommended HRP excitation reagent after 14 minutes of incubation. Each pair of dots and their intensity corresponds with the levels of phosphorylation of the respective kinase (listed in Figure 7 in the Materials and Methods). Note the difference in phosphorylation in the AKT S473 between mitoTERT and nucTERT*

in the Membrane B of the NUC and MITO transfected cells pointed by the black arrow. (n=1).

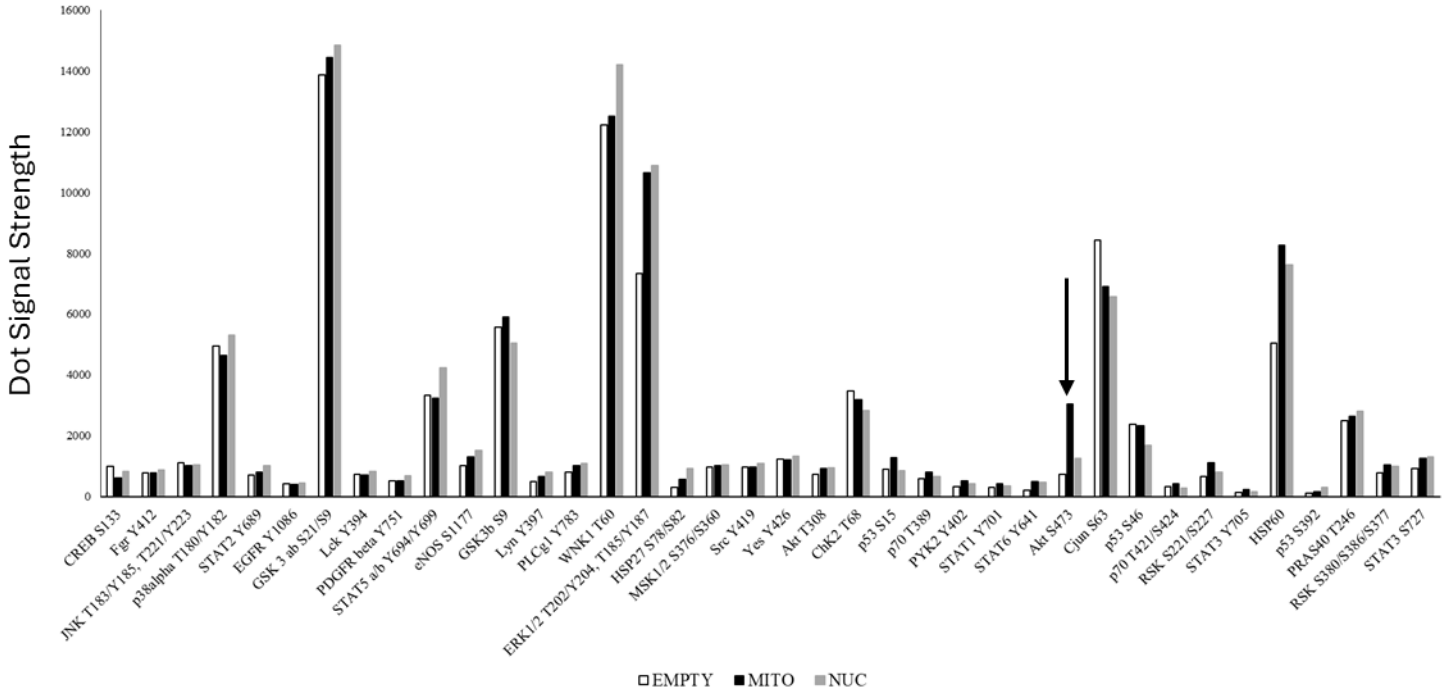

Figure 19: *Bar graph representing all signal levels of phosphorylated kinases (listed in Figure 7 in the Materials and Methods) present in K1 cells transfected with empty plasmid, mitoTERT and nucTERT, detected with the Human Phospho-Kinase Array kit. Note the difference in phosphorylation in AKT at the residue S473 between mitoTERT (black bar) and nucTERT (white bar) marked with the black arrow (n=1). On the Y-axis the signal the signal level strength detected from Membrane A and B with ImageJ.*

Mitochondrial TERT association with AKT activating phosphorylation, cell cycle arrest and DNA damage markers

We continued our research by confirming the results obtained with the kinase array by assaying the phosphorylation of AKT Ser473 by Western blot (P=0.04; n=3) [Figure 20].

Then, we wanted to expand our analysis by assaying cleaved PARP and

Caspase 3, p21 and γH2AX protein expression, as known markers of apoptosis, cell cycle arrest and DNA damage, in K1 cells transfected with nucTERT and mitoTERT.

p21 and γH2AX expression was found to be lower in cells transfected with mitoTERT compared to nucTERT (P=0.03 and 0.04, respectively; n=3) [Figure 21], while a trend toward reduced expression was observed for cleaved PARP and caspase 3, although the data did not reach statistical significance [Figure 22].

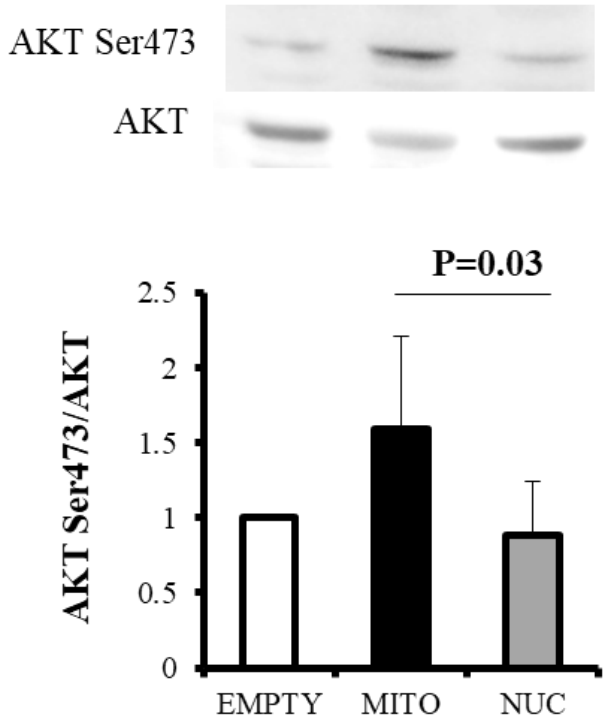

Figure 20: *Densitometry results of AKT ser 473 activating phosphorylation post-translational modification normalized with unmodified AKT protein expression. On the Y-axis is reported the ratio of signal strength of AKT phosphorylated over whole AKT protein expression.*

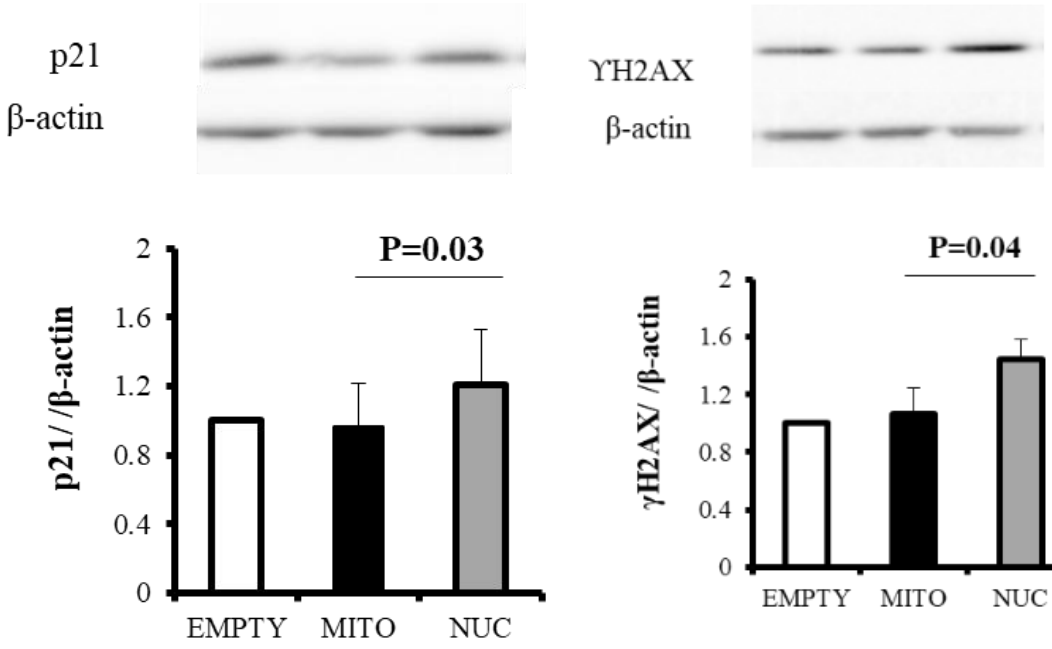

Figure 21: *Densitometry results of p21 and γH2AX protein expression normalized on the beta-actin protein expression. On the Y-axis is reported the ratio of signal strength of p21 over beta-actin expression used as a house-keeping control.*

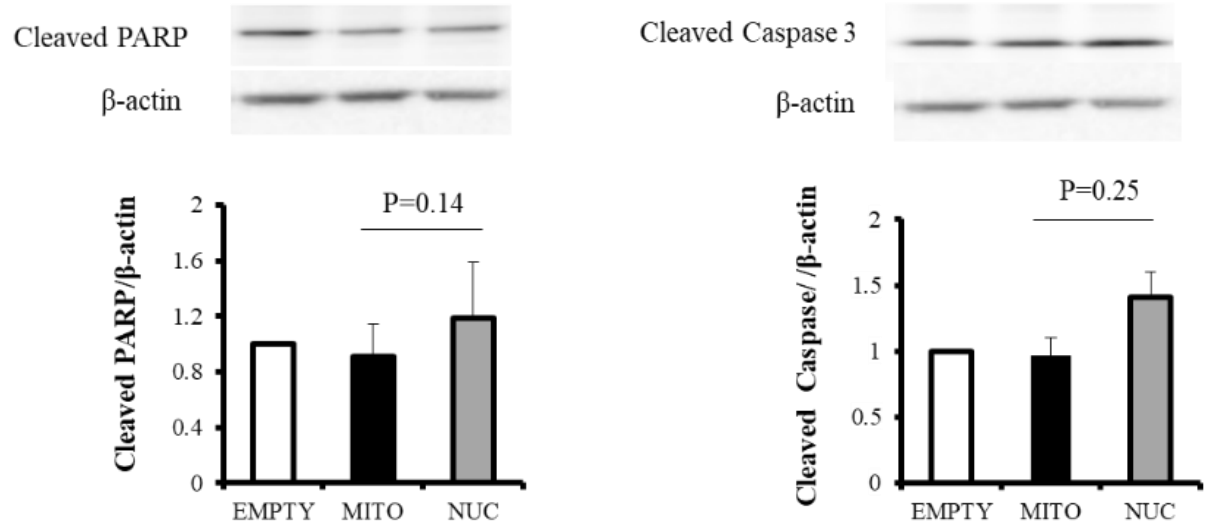

Figure 22: *Densitometry results of cleaved PARP and Cleaved Caspase-3 expression normalized on the beta-actin protein expression. On the Y-axis is reported the ratio of signal*

strength of cleaved PARP over beta-actin expression used as a house-keeping control.

TERT localization effect on OS, cell cycle arrest and outcome in PTC tissues

Finally, we concluded our investigation by assessing the TERT localization effects in 39 PTC tissues that have been previously genotyped in our lab through the PTC-MA assay [Table 3].

Sample	Age at diagnosis	Size (mm)	AJCC Stage	ETE	Multifo-cality	ATA risk	Persi-stence	Genetic profile
PTC1	64	20	II	Yes	Yes	Interme-diate	Yes	BRAFV600E+TERT-124
PTC2	71	11	II	Yes	No	High	Yes	BRAFV600E+TERT-124
PTC3	78	70	II	Yes	Yes	High	Yes	BRAFV600E+TERT-124
PTC4	50	21	I	No	No	Low	No	BRAFV600E
PTC5	42	19	II	No	No	Interme-diate	Yes	BRAFV600E
PTC6	25	23	I	Yes	Yes	Interme-diate	Yes	Ret/PTC3
PTC7	73	25	II	No	No	Interme-diate	No	WT
PTC8	65	32	I	No	No	Low	Yes	BRAFV600E
PTC9	17	70	I	Yes	Yes	Interme-diate	Yes	Ret/PTC1
PTC10	47	1	I	No	Yes	Interme-diate	No	NRASQ61K
PTC11	51	60	I	No	No	Low	No	BRAFV600E+TERT-124
PTC12	70	21	I	No	Yes	Interme-diate	No	BRAFV600E+TERT-124
PTC13	72	15	I	Yes	No	Low	No	BRAFV600E+TERT-124
PTC14	40	23	I	Yes	Yes	Interme-diate	Yes	WT
PTC15	13	5	I	No	No	Interme-diate	Yes	Ret/PTC1
PTC16	54	25	I	No	No	Low	Yes	BRAFV600E
PTC17	35	20	I	Yes	Yes	Interme-diate	Yes	BRAFV600E
PTC18	36	21	I	No	No	Low	Yes	Ret/PTC1
PTC19	28	3.8	I	No	Yes	Interme-diate	Yes	NRASQ61R
PTC20	58	5	I	No	No	Low	No	WT
PTC21	68	14	I	No	Yes	Low	Yes	WT
PTC22	58	21	II	No	Yes	Interme-diate	Yes	BRAFV600E
PTC23	50	12	I	No	No	Low	Yes	BRAFV600E
PTC24	51	12	I	No	No	Low	No	Ret/PTC1
PTC25	68	15	I	Yes	Yes	Low	No	WT
PTC26	77	44	II	Yes	Yes	Interme-diate	No	TERT-124
PTC27	40	7	I	Yes	No	Interme-diate	Yes	BRAFV600E
PTC28	76	14	I	No	No	Low	Yes	HRASQ61R
PTC29	52	7	I	No	No	Low	No	BRAFV600E
PTC 30	78	40	I	Yes	No	Low	Yes	BRAFV600E+TERT-124

PTC31	48	11	I	Yes	No	Low	No	BRAFV600E
PTC32	38	31	I	No	No	Low	Yes	WT
PTC33	43	22	I	No	No	Interme-diate	Yes	BRAFV600E
PTC34	30	12	I	No	No	Low	No	BRAFV600E
PTC35	40	8	I	No	No	Low	No	BRAFV600E
PTC36	38	7	I	No	No	Low	No	BRAFV600E
PTC37	58	11	I	No	No	Low	No	BRAFV600E
PTC38	28	40	I	Yes	Yes	Interme-diate	Yes	WT
PTC39	53	7	I	No	Yes	Low	No	BRAFV600E

Table 3: *Genetic and clinicopathological characteristics of patients for the study. Genetic characterisation of the tissues was performed by PTC-MA Mass ARRAY analysis. Clinicopathological data was collected and reviewed by expert clinicians*.

TERT localization was assayed by Western Blot on proteins obtained after tissue fractionation. Most tissues showed both nuclear and mitochondrial TERT localization [Figure 23]. Given the variability of TERT expression in the tumors analyzed, TERT mitochondrial/nuclear ratio was then correlated with clinicopathological characteristics of the patients, with the oxidative stress found in the tissues, evaluated by Amplex-Red probe, and with, p21, γH2AX and cleaved PARP protein expression, assayed by Western Blot.

Interestingly, the ratio of mitochondrial over nuclear TERT expression resulted significantly correlated with tumor persistence (P=0.02; n=3) [Figure 24]. Moreover, the TERT mitochondrial/nuclear ratio was inversely correlated with OS measured in the tissues (P=0.02; n=3) [Figure 24]. In addition, p21 expression was associated to OS found in the tissues analyzed (P=0.007; n=3) and inversely correlated to the mitochondrial/nuclear TERT ratio (P=0.03; n=3) [Figure 25]. Finally, no significant correlation was found between TERT mitochondrial/nuclear ratio and γH2AX or cleaved PARP [Figure 26].

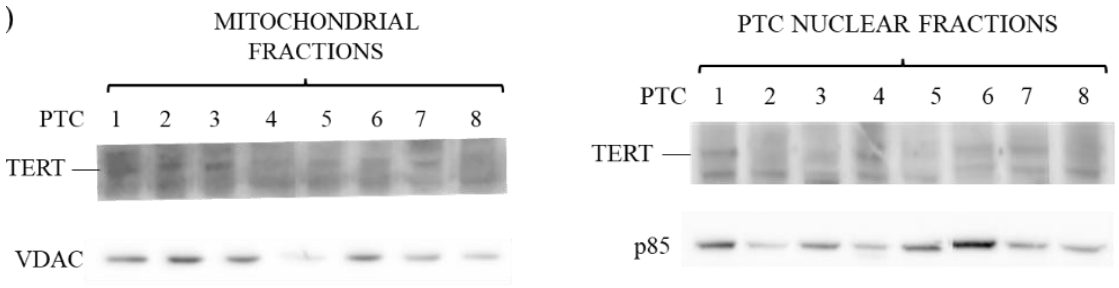

Figure 23: *Representative images of western blots of TERT protein localization assayed in mitochondrial and nuclear fractions.*

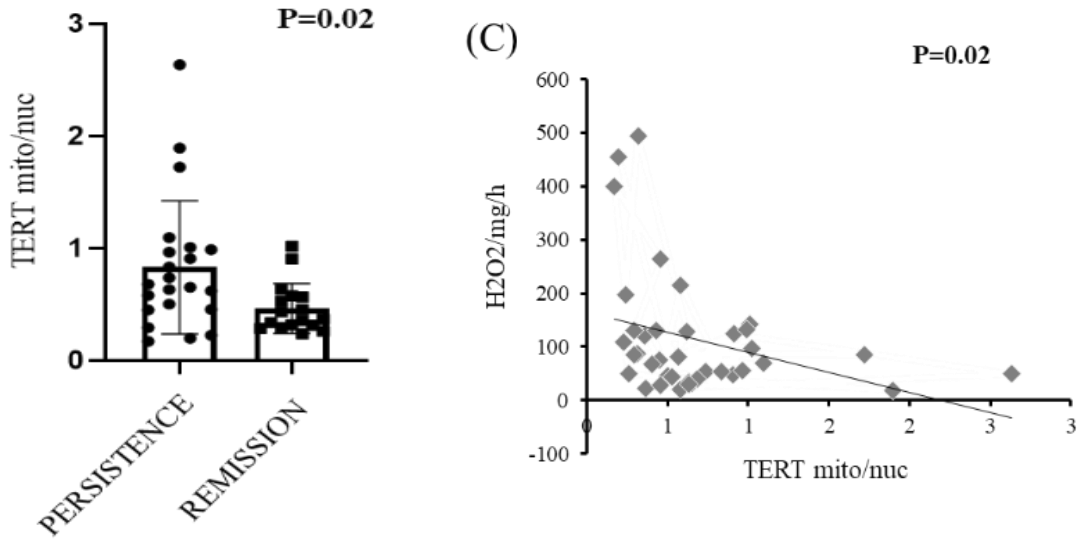

Figure 24: *Bar graphs representing the correlation between TERT mitochondrial over nuclear ratio with persistence and H_2O_2 found in the tissues (Left panel and Right panel).*

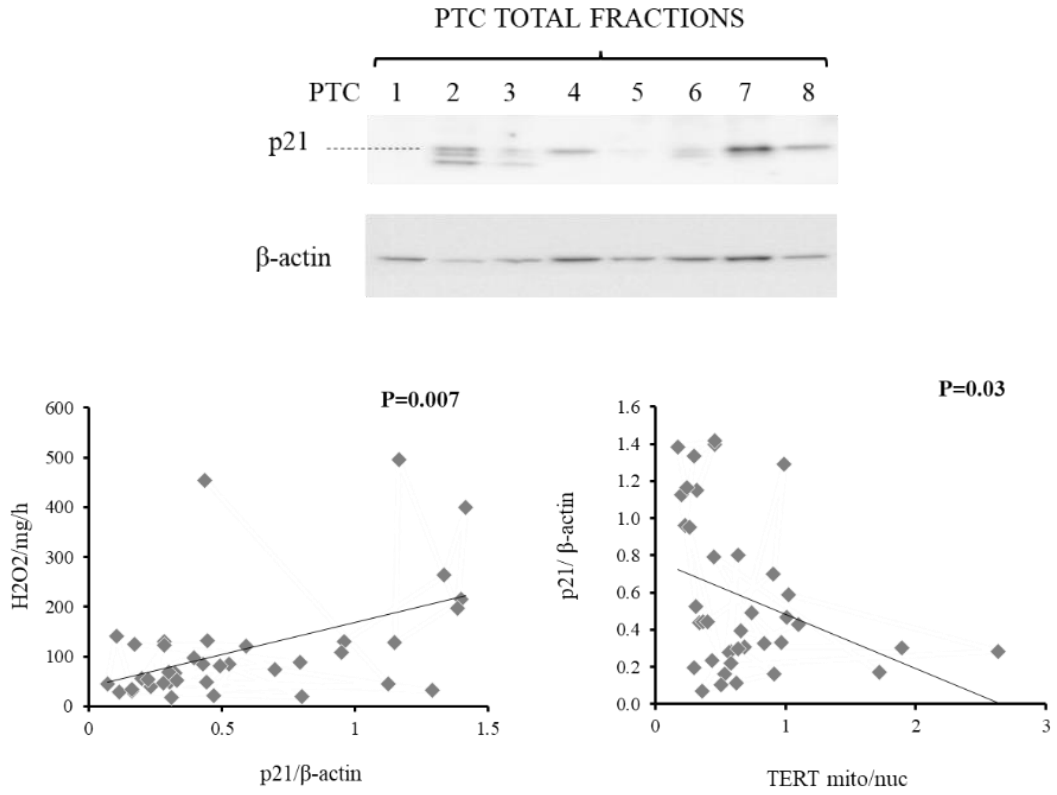

Figure 25: *p21 protein expression in PTC total fractions normalized by beta actin expression (Above). Correlation between p21 protein expression with H_2O_2 found in the tissue and TERT mitochondrial/nuclear ratio (Left panel and right panel).*

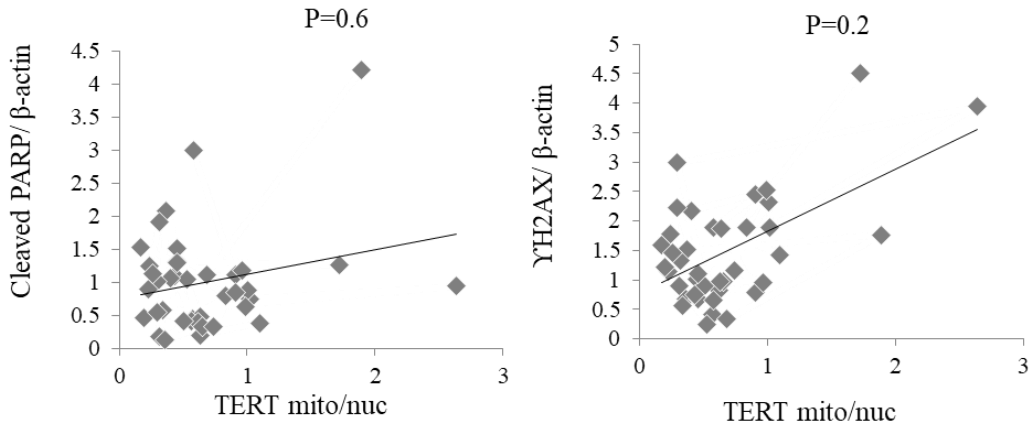

Figure 26: *Correlation between cleaved PARP or γH2AX expression and TERT mitochondrial/nuclear ratio (Left panel and right panel). No significant correlation was found.*

Discussion

Papillary thyroid cancer (PTC) is the most common form of endocrinological neoplasm in the world with an increasing incidence reported over the years. In around 10-15% of cases PTC can display aggressive behavior. For these cases, treatment with tyrosine kinase inhibitors (TKIs) inhibiting the MAPK pathway has been approved and is currently in use. Nevertheless, some tumors are/become resistant to these compounds, through mechanisms still not fully understood, suggesting the existence or development of compensatory mechanisms [57].

The role of TERT has been recognized over the years as a useful prognostic marker of aggressiveness and response to therapy, although the mechanism of action through which these effects are produced has not be clearly elucidated, further complicated by the different sub-compartmental localizations reported in the literature [38,39,41,42,45,46,49,58].

In accordance with this information, it is no surprise that the telomerase is been considered an interesting therapeutic target for cancers. A number of therapies have been developed and can be broadly classified in direct telomerase inhibitors, indirect telomerase inhibitors and anti-TERT immunotherapies. Direct telomerase inhibitors target TERT directly by binding to it such as BIBR1532, MST-312, MST-199 and Imetelstat. Indirect telomerase inhibitors work by binding to other proteins implicated in the TERT pathway such as geldanamycin that works by inhibiting HSP90, an important chaperone for maintaining proper telomerase activity or G-quadruplex stabilizers, molecules capable of strengthening these secondary structures that form on telomere sequences, that were capable of reducing tumor growth in leukemia xenograft models [65]. Anti-TERT immunotherapies have been developed once it was understood that TERT peptides can be recognized by MHC class I and II and trigger an immune response; examples of this class of anti-TERT therapies are vaccines, adoptive cell transfer and oncolytic virotherapy. An example of

vaccine is GV1001 that reached phase III clinical trials in patients with advanced pancreatic cancer. The main challenge for these treatments is the poor clinical efficacy, perhaps due to low potency or the lack of prior selection for patients with high TERT expression. TERT targeting by synthetic compounds is also complicated by high cytotoxicity [66,67,68]

To this date there are no reports of anti-TERT therapies aimed for advanced cases of papillary thyroid carcinomas despite hTERT promoter mutations have been reported in these cases.

In this work, we aimed to dissect the role of TERT localization in response to exogenously simulated oxidative stress and more specifically, the role of mitochondrial TERT in increasing aggressive characteristics and progression in papillary thyroid cancer, hopefully unmasking further molecular mechanisms that may be targeted with more effectiveness than currently available therapies.

The K1 cell line was selected among the different thyroid cancer cell lines available due to its genotypical characteristics that most closely resembles those of a classical aggressive papillary thyroid cancer case, namely: presence of BRAF V600E mutation, absence of TP53 variants and a diploid and microsatellite stable genome.

K1 cells transfected with the TERT WT plasmid, in untreated conditions, exhibited a frequent and expected nuclear signal, consistent with the classical function of TERT at the telomere level. Rarely and more frequently when cells are challenged with hydrogen peroxide, the pattern of expression of TERT was found to be more cytoplasmatic and in some cases a colocalization signal with the mitochondria was detected. Cytoplasmic and mitochondrial localization of TERT have been previously reported in other cell lines and human cancers, as a response to increased stress levels in the cell [41,45,46,49,58].

To confirm and quantify this phenomenon, we counted the number of TERT expression patterns in cells in untreated and H_2O_2-challenged conditions as commonly reported in the literature and with treatment of the BRAF-inhibitor

PLX4720, that we showed to impact the stress levels of thyroid cancer cells. Indeed, TERT localization shift from the nucleus to the cytoplasm was observed for the first time in thyroid cancer cells in H_2O_2 treated conditions, as expected. This same behavior could be replicated, although with less statistical significance, in PLX4720 treated cells.

Our analysis of the confocal images also showed an interesting fragmentation pattern of the mitochondria in TERT transfected cells. Indeed, our further investigation on mitochondrial dynamics with the Fiji software showed a reduction in all parameters, consistent with the pattern of mitochondrial fission. Mitochondrial fission is a process involved in mitophagy to remove damaged mitochondria and preserve cancer cells from excessive OS [59], thus inducing resistance toward pro-oxidant compounds, such as PLX4720. Interestingly, either in basal or stress conditions induced by H_2O_2 or PLX4720, extra-nuclear TERT was associated to a higher mitochondrial fragmentation than nuclear TERT, indicating its role in mitophagy, as previously observed [ref 28 paper]. Mitochondrial dynamics also have an important role in the metabolism of cells and importantly in cancer cells. In particular, mitochondrial fragmentation has relevance for processes like apoptosis and glycolysis and has been widely reported as marker for aggressiveness in many tumor types.

We then decided to study the effect of TERT on the actual OS produced by the mitochondria, this being an important stress marker for cancer cells under proliferative and metabolic stress. We found a remarkable reduction of mitochondrial ROS in TERT transfected cells when it was located in the extra-nuclear compartments. This result is consistent with the previous literature findings that TERT ameliorates ROS generation [58]. The reduction in ROS levels could be mechanistically linked with increased mitochondrial fission by the process of mitophagy that has been recently associated to a specific interaction between hTERT and PINK1 [54].

We then decided to employ the use of localization limited TERT plasmids to

further dissect the roles of TERT, without further stressing cells with the addition of H_2O_2. With the help of these plasmids, we studied the proliferation, invasion and glycolysis processes. We found that mitochondrial TERT was capable of improving all three characteristics in a statistically significant manner compared to TERT expressed only in the nucleus. This result in thyroid cancer cells could be consistent with the previous literature on TERT increasing glycolytic metabolism and other aggressive characteristics [60,61]. These results were also coherent with our data showing a strong correlation between TERT extra-nuclear expression and mitochondrial fission, a condition that has been previously associated with greater glycolysis dependence, given the reduced ability for OXPHOS metabolism [62].

To reinforce our results, we decided to test the capabilities of PP2, a Src Kinase inhibitor that should functionally block TERT export from the nucleus. Indeed, PP2 was capable of reducing proliferation, invasion and glycolysis, all parameters that were enhanced by mitochondrial TERT transfection.

Unfortunately, this effect cannot be explained only through its action on the TERT export, as Src kinase is involved in many different cellular processes. However, this result may give more insights into the therapeutic effect of manipulating TERT export, rather than inhibiting it wholesale as it may cause important side effects [42,63].

As Src has been found to be a key regulator in many cellular processes from glucose uptake and cellular bioenergetics to cell adhesion, migration and invasion, PP2 and dabrafenib have been extensively in used translational research for targeting pancreatic cancer stem cells, reversion of stemness in glioblastoma cells and reduced proliferation in liver cancer cells. PP2 and Src kinase inhibitors were tested on PTC cells by Henderson and colleagues where they have shown promise in reducing cell proliferation, although not changing the survival of the in vivo mouse model at their disposal, perhaps suggesting that Src inhibitors should be used in combination therapies to reach a more

satisfactory therapeutic effect [69,70].

We continued our studies by assessing some markers of aggressiveness, namely γH2AX and p21 as markers of DNA damage and senescence, finding them both downregulated in cells transfected with mitochondrial TERT. We interpreted this result as a beneficial effect as the effect of mitochondrial TERT for cell stress. Indeed, both γH2AX which is a marker of nuclear DNA damage, and p21, which promotes cell cycle arrest in response to many stimuli, including OS and DNA damage [64] were found increased in cells with the nuclear TERT localization.

Finally, we considered evaluating the role of hTERT in causing different phosphorylation of key targets in many proliferation, survival and cancer-related pathways. Among the different phosphorylated proteins, p-AKT phosphorylation at the Serine in position 473 (S473) showed the highest difference between different TERT localizations. S473 is a key phosphorylated residue on Akt that is correlated to its activation. Activation of Akt is at the center of multiple pathways integrating cell proliferation, survival, metastasis and metabolic shifting towards metabolism [Figure 27]. This result was consistent with the increase of proliferation, invasion and glycolysis associated to mitochondrial TERT, observed in previous experiments.

To give more depth to the study we decided to evaluate TERT localization in PTC frozen and correlate to relevant clinico-pathological information of the patients. Our experiments revealed that the fraction of TERT mitochondrial/nuclear localization was correlated with reduced OS and p21 protein expression levels, consistent with our previous results obtained in in-vitro model. Moreover, a higher mitochondrial/nuclear TERT rate resulted associated with tumor persistence. These results delineate an interaction between mitochondrial TERT localization, ROS production management and cell stress reduction, and thyroid cancer aggressiveness.

Our findings obtained in thyroid cancer cells and tissues indicate that TERT has

different and important actions in different sub-compartments, important for the maintenance of many hallmarks of cancer. Limiting TERT expression to the classical nuclear compartment is capable of reducing some of these characteristics. For this purpose, nuclear export inhibitors might provide a different therapeutic avenue that may limit oncogenic potential without overly compromising the normal tissue.

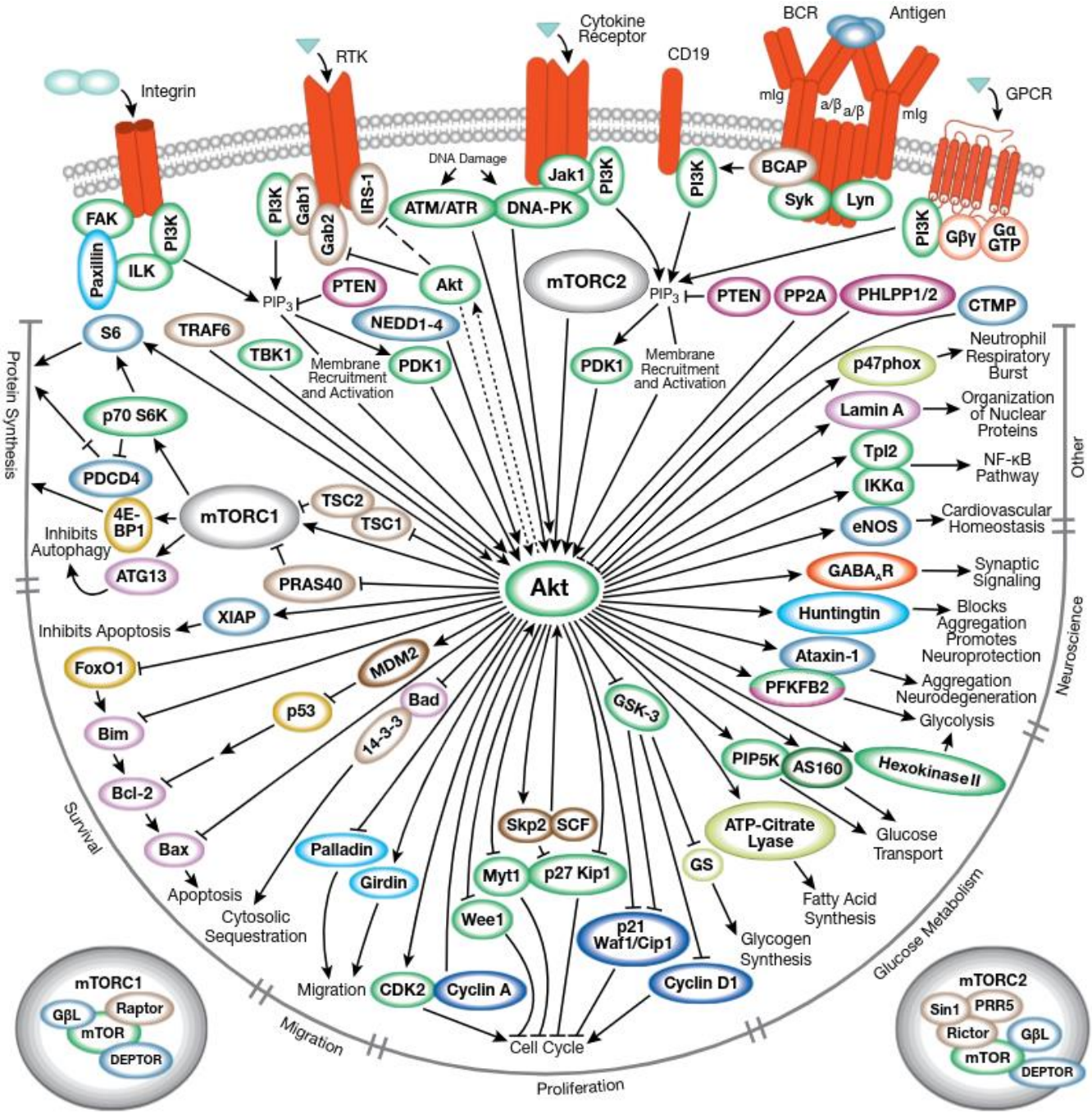

Figure 27: *Scheme of Akt signaling in cancer involving survival, migration, proliferation and glucose metabolism pathways (image taken from Cell Signaling Technologies website).*

Limitations of the study and future perspectives

The primary limitation of this study is inherent to the in-vitro model used in this work. Transient transfection is difficult to achieve in thyroid cancer cell lines. Furthermore, transient transfection compared to stable transfection tends to significantly increase expression of the protein target of the study. Transient overexpression was our solution to the low expression of TERT, an issue compounded by the known unreliability of available TERT antibodies. This limitation was particularly relevant in tissue fractionation experiments, a process that inherently reduces the concentration of target proteins, requiring great care in sample collection to waste as little material as possible.

In the future we believe that implementing a stable transfection of hTERT plasmid with an added FLAG tag could facilitate localization experiments and increase general throughput of experiments.

Another issue with the model is the use of only the K1 thyroid cell line, although they are the only cell lines that maintain the genotype of an advanced papillary thyroid carcinoma without TP53 mutations, that more closely define poorly differentiated thyroid carcinomas.

A different strategy could be employing primary cell cultures of advanced papillary thyroid cancer. The main advantages of this approach would be the availability of cells of the same subtype, without carrying the issue of immortalized cell lines that drift away from the classical genotype.

Another limitation of the study is the lack of advanced techniques used for many analyses. Employing electric microscopy or super-resolution confocal microscopy could give more reliable and in-depth results in localization and mitochondrial imaging. Use of the Seahorse XF Analyzer (Agilent) and its real-time metabolic kits could also be an interesting and high throughput technique to evaluate many mitochondrial stress markers and possibly test out different treatment conditions at the same time.

It is interesting to note that reported TERT copies in cancer cells are very few,

so it would be fruitful to know the status and health of the telomeres under stress conditions while TERT expresses its action at the mitochondrial level. In this context, studying the alternative lengthening of telomeres (ALT) process might elucidate a possibly important pathway that allows TERT to exit the nucleus without causing damage to the cell.

Conclusions

Oxidative stress could represent an interesting new pathway in the study of thyroid tumor pathogenesis and progression.

We confirmed in our in-vitro and tissue protein expression studies that TERT is exported to the cytoplasm and in part in the mitochondria in response to exogenous stress increase, and that mitochondrial TERT increases the cell capabilities of managing oxidative stress. This mechanism can be considered important in maintaining thyroid cancer's aggressive abilities such as proliferation, invasion and glycolysis, all processes that cause sharp increases in ROS production and related DNA damage and cell cycle arrest.

While not directly explored in our work, TERT extra-nuclear properties may also represent a mechanism of resistance to treatment with tyrosine kinase inhibitors commonly used in medical practice, since vemurafenib was shown to also increase oxidative stress levels in K1 cells.

We successfully tested the SRC kinase inhibitor PP2 as a possible treatment that can inhibit TERT nuclear export and that was capable of impacting cell proliferation, migration, and glycolytic capacity in K1 cells. However, SRC kinase is a key enzyme in many pathways responsible for cancer growth and proliferation and so far as this work is concerned, we cannot pin its effect only on TERT. A better understanding of the complete process responsible for TERT nuclear export is required to develop more specific treatment for future therapeutic targeting. Indeed, we believe that inhibiting the TERT nuclear

export pathway may provide a beneficial effect in reducing both cancer cell resistance to oxidative stress and aggressive characteristics that are common in treatment-resistant advanced PTCs.

References:

1. Rahbari R, Zhang L, and Kebebew E. **Thyroid cancer gender disparity.** Future Oncol. 2010; 6(11): 1771–1779. doi: 10.2217/fon.10.127

2. Baloch ZW, Asa SL, Barletta JA et al. **Overview of the 2022 WHO Classification of Thyroid Neoplasms.** Endocr Pathol. 2022;33(1):27-63. doi: 10.1007/s12022-022-09707-3.

3. Noone A, Cronin KA, Altekruse SF et al. **Cancer Incidence and Survival Trends by Subtype Using Data from the Surveillance Epidemiology and End Results Program, 1992-2013.** Cancer Epidemiol Biomarkers Prev. 2017;26(4):632-641. doi: 10.1158/1055-9965.EPI-16-0520.

4. Deng Y, Li H, Wang M, et al. **Global Burden of Thyroid Cancer From 1990 to 2017.** JAMA Netw Open. 2020;3(6):e208759. doi:10.1001/jamanetworkopen.2020.8759

5. Kitahara CM and Schneider AB. **Cancer Progress and Priorities: Epidemiology of Thyroid Cancer.** Cancer Epidemiol Biomarkers Prev. 2022 Jul 1; 31(7): 1284–1297.doi: 10.1158/1055-9965.EPI-21-1440

6. Cirello V, Lugaresi M, Fugazzola L et al. **Thyroid cancer and endocrine disruptive chemicals: a case-control study on perfluoroalkyl substances (PFAS) and other persistent organic pollutants (POPs).** Eur. Thyroid J. 2023 (forthcoming)

7. Maniakas A, Dadu R, Busaidy NL, et al. **Evaluation of Overall Survival in Patients With Anaplastic Thyroid Carcinoma, 2000-2019.** JAMA Oncol. 2020 Sep 1;6(9):1397-1404. doi: 10.1001/jamaoncol.2020.3362.

8. Prete A, Matrone A, Gambale C, et al. **Poorly Differentiated and Anaplastic Thyroid Cancer: Insights into Genomics Microenvironment and New Drugs.** Cancers (Basel). 2021;13(13):3200. doi: 10.3390/cancers13133200.

9. Links TP, van Tol KM, Jager PL, et al. **Life expectancy in differentiated thyroid cancer: a novel approach to survival analysis.** Endocr Relat Cancer.

2005 Jun;12(2):273-80. doi: 10.1677/erc.1.00892.

10. Haddad RI, Bischoff L, Ball D, et al. **Thyroid Carcinoma, Version 2.2022, NCCN Clinical Practice Guidelines in Oncology.** J Natl Compr Canc Netw. 2022;20(8):925-951. doi: 10.6004/jnccn.2022.0040.

11. Manzil FFP, Kaur H. **Radioactive Iodine for Thyroid Malignancies.** Treasure Island (FL): StatPearls Publishing; 2023.

12. Puliafito I, Esposito F, Prestifilippo A et al. **Target Therapy in Thyroid Cancer: Current Challenge in Clinical Use of Tyrosine Kinase Inhibitors and Management of Side Effects.** Front Endocrinol (Lausanne). 2022; 8:13:860671. doi: 10.3389/fendo.2022.860671.

13. Pesenti C, Muzza M, Colombo C et al. **MassARRAY-based simultaneous detection of hotspot somatic mutations and recurrent fusion genes in papillary thyroid carcinoma: the PTC-MA assay.** Endocrine. 2018;61(1):36-41. doi: 10.1007/s12020-017-1483-2

14. Colombo C, Muzza M, Proverbio MC et al. **Impact of Mutation Density and Heterogeneity on Papillary Thyroid Cancer Clinical Features and Remission Probability.** Thyroid. 2019;29(2):237-251. doi: 10.1089/thy.2018.0339.

15. Colombo C, Muzza M, Pogliaghi G et al. **The thyroid risk score (TRS) for nodules with indeterminate cytology.** Endocr Relat Cancer. 2021;28(4):225-235. doi: 10.1530/ERC-20-0511.

16. Lam AK. **Papillary Thyroid Carcinoma: Current Position in Epidemiology, Genomics, and Classification.** Methods Mol Biol. 2022:2534:1-15. doi: 10.1007/978-1-0716-2505-7_1.

17. *American Cancer Society.* **Thyroid Cancer Survival Rates, by Type and Stage, american cancer society.** https://www.cancer.org/cancer/types/thyroid-cancer/detection-diagnosis staging/survival-rates.html

18. Ruegemer JJ, Hay ID, Bergstralh EJ, Ryan JJ, Offord KP et al. **Distant**

metastases in differentiated thyroid carcinoma: a multivariate analysis of prognostic variables. J Clin Endocrinol Metab. 1988;67(3):501-8. doi: 10.1210/jcem-67-3-501.

19. Fullmer T, Cabanillas ME, Zafereo M. **Novel Therapeutics in Radioactive Iodine-Resistant Thyroid Cancer.** Front Endocrinol (Lausanne). 2021; 15:12:720723. doi: 10.3389/fendo.2021.720723.

20. Aashiq M, Silverman DA, Na'ara S, et al. **Radioiodine-Refractory Thyroid Cancer: Molecular Basis of Redifferentiation Therapies, Management, and Novel Therapies.** Cancers (Basel). 2019; 11(9):1382. doi: 10.3390/cancers11091382.

21. Bonora E, Tallini G, Romeo G. **Genetic Predisposition to Familial Nonmedullary Thyroid Cancer: An Update of Molecular Findings and State-of-the-Art Studies.** J Oncol. 2010:2010:385206. doi: 10.1155/2010/385206.

22. Capezzone M, Robenshtok E, Cantara S et al. **Familial non-medullary thyroid cancer: a critical review.** J Endocrinol Invest. 2021;44(5):943-950. doi: 10.1007/s40618-020-01435-x.

23. Juhlin CC, Mete O, Baloch ZW. **The 2022 WHO classification of thyroid tumors: novel concepts in nomenclature and grading.** Endocr Relat Cancer. 2022; 30(2):e220293. doi: 10.1530/ERC-22-0293.

24. Cancer Genome Atlas Research Network. **Integrated genomic characterization of papillary thyroid carcinoma.** Cell. 2014; 159(3):676-90. doi: 10.1016/j.cell.2014.09.050.

25. Sholl LM. **A narrative review of BRAF alterations in human tumors: diagnostic and predictive implications.** Precision Cancer Medicine. 2020:3.

26. Prior IA, Lewis PD, Mattos C. **A comprehensive survey of Ras mutations in cancer.** Cancer Res. 2012; 15;72(10):2457-67. doi: 10.1158/0008-5472.CAN-11-2612.

27. Vinagre J, Almeida A, Pópulo H et al. **Frequency of TERT promoter**

mutations in human cancers. Nat Commun. 2013:4:2185. doi: 10.1038/ncomms3185.

28. Ciampi R, Nikiforov YE. **RET/PTC Rearrangements and BRAF Mutations in Thyroid Tumorigenesis.** Endocrinology. 2007; 148(3):936-41. doi: 10.1210/en.2006-0921.

29. Pekova B, Sykorova V, Mastnikova K et al. **NTRK Fusion Genes in Thyroid Carcinomas: Clinicopathological Characteristics and Their Impacts on Prognosis.** Cancers (Basel). 2021 16;13(8):1932. doi: 10.3390/cancers13081932.

30. Raman P, Koenig RJ. **Pax-8–PPAR-γ fusion protein in thyroid carcinoma.** Nat Rev Endocrinol. 2014;10(10):616-23. doi: 10.1038/nrendo.2014.115.

31. Perillo B, Di Donato M, Pezone A et al. **ROS in cancer therapy: the bright side of the moon.** Exp Mol Med. 2020;52(2):192-203. doi: 10.1038/s12276-020-0384-2.

32. El Hassani RA, Buffet C, Leboulleux S, et al. **Oxidative stress in thyroid carcinomas: biological and clinical significance.** Endocr Relat Cancer. 2019; 26(3):R131-R143.doi: 10.1530/ERC-18-0476.

33. Kochman J, Jakubczyk K, Bargiel P et al. **The Influence of Oxidative Stress on Thyroid Diseases.** Antioxidants (Basel). 2021; 10;10(9):1442. doi: 10.3390/antiox10091442.

34. Carvalho DP, Dupuy C. **Role of the NADPH Oxidases DUOX and NOX4 in Thyroid Oxidative Stress.** Eur Thyroid J. 2013;2(3):160-7. doi: 10.1159/000354745.

35. Weyemi U, Caillou B, Talbot M, et al. **Intracellular expression of reactive oxygen species-generating NADPH oxidase NOX4 in normal and cancer thyroid tissues.** Endocr Relat Cancer. 2010. 17(1):27-37. doi: 10.1677/ERC-09-0175.

36. Azouzi N, Cailloux J, Cazarin JM, et al. **NADPH Oxidase NOX4 Is a Critical**

Mediator of BRAF V600E-Induced Downregulation of the Sodium/Iodide Symporter in Papillary Thyroid Carcinomas. Antioxid Redox Signal. 2017. 26(15):864-877.doi: 10.1089/ars.2015.6616.

37. Muzza M, Pogliaghi G, Colombo C et al. **Oxidative Stress Correlates with More Aggressive Features in Thyroid Cancer.** Cancers (Basel). 2022 28;14(23):5857. doi: 10.3390/cancers14235857.

38. Ségal-Bendirdjian E, Geli V. **Non-canonical Roles of Telomerase: Unraveling the Imbroglio.** Front Cell Dev Biol. 2019;10:7:332. doi: 10.3389/fcell.2019.00332. eCollection 2019.

39. Dratwa M, Wysoczańska B, Łacina P. **TERT—Regulation and Roles in Cancer Formation.** Front Immunol. 2020;19:11:589929. doi: 10.3389/fimmu.2020.589929.

40. Fragkiadaki P, Renieri E, Kalliantasi K et al. **Telomerase inhibitors and activators in aging and cancer: A systematic review.** Mol Med Rep. 2022;25(5):158. doi: 10.3892/mmr.2022.12674.

41. Chiodi I, Mondello C**. Telomere-independent functions of telomerase in nuclei, cytoplasm, and mitochondria.** Front Oncol. 2012;28:2:133. doi: 10.3389/fonc.2012.00133.

42. Romaniuk A, Paszel-Jaworska A, Totoń E et al.**The non-canonical functions of telomerase: to turn off or not to turn off.** Mol Biol Rep. 2019;46(1):1401-1411. doi: 10.1007/s11033-018-4496-x.

43. Cheng Y, Liu P, Zheng Q et al**. Mitochondrial Trafficking and Processing of Telomerase RNA TERC.** Cell Rep. 2018 4;24(10):2589-2595. doi: 10.1016/j.celrep.2018.08.003.

44. Liu H, Yang Y, Ge Y et al. **TERC promotes cellular inflammatory response independent of telomerase.** Nucleic Acids Res. 2019 5;47(15):8084-8095. doi: 10.1093/nar/gkz584.

45. Marinaccio J, Micheli E, Udroiu I et al. **TERT Extra-Telomeric Roles: Antioxidant Activity and Mitochondrial Protection.** Int J Mol Sci. 2023 23;24(5):4450. doi: 10.3390/ijms24054450.

46. Haendeler J, Hoffmann J, Brandes RP, et al. **Hydrogen Peroxide Triggers**

Nuclear Export of Telomerase Reverse Transcriptase via Src Kinase Family-Dependent Phosphorylation of Tyrosine 707. Mol Cell Biol. 2003; 23(13):4598-610.doi: 10.1128/MCB.23.13.4598-4610.2003.

47. Jakob S, Schroeder P, Lukosz M, et al. **Nuclear protein tyrosine phosphatase Shp-2 is one important negative regulator of nuclear export of telomerase reverse transcriptase.** J Biol Chem. 2008. 283(48):33155-61.doi: 10.1074/jbc.M805138200

48. Santos JH, Meyer JN, Skorvaga M et al. **Mitochondrial hTERT exacerbates free-radical-mediated mtDNA damage.** Aging Cell. 2004;3(6):399-411. doi: 10.1111/j.1474-9728.2004.00124.x.

49. Haendeler J, Drose S, Buchner N, et al. **Mitochondrial Telomerase Reverse Transcriptase Binds to and Protects Mitochondrial DNA and Function From Damage.** Arterioscler Thromb Vasc Biol. 2009. 29(6):929-35.doi: 10.1161/ATVBAHA.109.185546.

50. Sharma S, Mukherjee AK, Roy SS et al. **Human telomerase is directly regulated by non-telomeric TRF2-G-quadruplex interaction.** Cell Rep. 2021;18;35(7):109154. doi: 10.1016/j.celrep.2021.109154.

51. Gordon DM, Santos JH. **The Emerging Role of Telomerase Reverse Transcriptase in Mitochondrial DNA Metabolism.** J Nucleic Acids. 2010;21:2010:390791. doi: 10.4061/2010/390791.

52. Valente AJ, Maddalena LA, Robb EL et al. **A simple ImageJ macro tool for analyzing mitochondrial network morphology in mammalian cell culture.** Acta Histochem. 2017;119(3):315-326. doi: 10.1016/j.acthis.2017.03.001.

53. Lucarelli G, Rutigliano M, Loizzo D et al. **MUC1 Tissue Expression and Its Soluble Form CA15-3 Identify a Clear Cell Renal Cell Carcinoma with Distinct Metabolic Profile and Poor Clinical Outcome.** Int J Mol Sci. 2022;12;23(22):13968. doi: 10.3390/ijms232213968.

54. Shin WH, Chung KC. **Human telomerase reverse transcriptase**

positively regulates mitophagy by inhibiting the processing and cytoplasmic release of mitochondrial PINK1. Cell Death Dis. 2020;8;11(6):425. doi: 10.1038/s41419-020-2641-7.

55. Rai Y, Pathak R, Kumari N et al. **Mitochondrial biogenesis and metabolic hyperactivation limits the application of MTT assay in the estimation of radiation induced growth inhibition.** Sci Rep. 2018;24;8(1):1531. doi: 10.1038/s41598-018-19930-w.

56. Trotta AP, Chipuk JE. **Mitochondrial Dynamics As Regulators Of Cancer Biology.** Cell Mol Life Sci. 2017;74(11):1999-2017. doi: 10.1007/s00018-016-2451-3.

57. Fugazzola L, Elisei R, Fuhrer D et al. **2019 European Thyroid Association Guidelines for the Treatment and Follow-Up of Advanced Radioiodine-Refractory Thyroid Cancer.** Eur Thyroid J. 2019;8(5):227-245. doi: 10.1159/000502229.

58. Indran IR, Hande MP, Pervaiz S. **hTERT overexpression alleviates intracellular ROS production, improves mitochondrial function, and inhibits ROS-mediated apoptosis in cancer cells.** Cancer Res. 2011;1;71(1):266-76. doi: 10.1158/0008-5472.CAN-10-1588.

59. Boulton DP, Caino MC. **Mitochondrial Fission and Fusion in Tumor Progression to Metastasis.** Front Cell Dev Biol. 2022;10:849962. doi: 10.3389/fcell.2022.849962.

60. Viswanath P, Batsios G, Ayyappan V et al. **Metabolic imaging detects elevated glucose flux through the pentose phosphate pathway associated with TERT expression in low-grade gliomas.** Neuro Oncol. 2021;1;23(9):1509-1522. doi: 10.1093/neuonc/noab093.

61. Bonuccelli G, Peiris-Pages M, Ozsvari B et al. **Targeting cancer stem cell propagation with palbociclib, a CDK4/6 inhibitor: Telomerase drives tumor cell heterogeneity.** Oncotarget. 2017;7;8(6):9868-9884. doi: 10.18632/oncotarget.14196.

62. Punter KB, Chu C, Chan EYW. **Mitochondrial dynamics and oxidative phosphorylation as critical targets in cancer.** Endocr Relat Cancer. 2022;30(1):e220229. doi: 10.1530/ERC-22-0229.

63. Ait-Aissa K, Ebben JD, Kadlec AO et al. **Friend or Foe? Telomerase as a Pharmacological target in Cancer and Cardiovascular Disease.** Pharmacol Res. 2016:111:422-433. doi: 10.1016/j.phrs.2016.07.003.

64. Abbas T, Dutta A. **p21 in cancer: intricate networks and multiple activities.** Nat Rev Cancer. 2009;9:400-414. doi: 10.1038/nrc2657.

65. Fragkiadaki P, Renieri E, Kalliantasi K et al. **Telomerase inhibitors and activators in aging and cancer: A systematic review.** Mol Med Rep. 2022 May; 25(5): 158. doi: 10.3892/mmr.2022.12674

66. Guterres AN, Jessie Villanueva J.**Targeting telomerase for cancer therapy.** Oncogene. 2020 Sep;39(36):5811-5824. doi: 10.1038/s41388-020-01405-w.

67. Ivancich M, Schrank Z, Wojdyla L et al.**Treating Cancer by Targeting Telomeres and Telomerase.** Antioxidants (Basel). 2017 Feb 19;6(1):15. doi: 10.3390/antiox6010015.

68. Yan S, Lin S, Qiu H et al. **Regulation of telomerase towards tumor therapy.** Cell Biosci. 2023 Dec 18;13(1):228. doi: 10.1186/s13578-023-01181-6.

69. Henderson YC, Toro-Serra R, Chen Y et al. **Src Inhibitors Suppress the Growth of Papillary Thyroid Carcinoma.** Head Neck. 2014 Mar;36(3):375-84. doi: 10.1002/hed.23316.

70. Pelaz SG, Tabernero A. **Src: coordinating metabolism in cancer.** Oncogene. 2022 Nov;41(45):4917-4928. doi: 10.1038/s41388-022-02487-4.

Acknowledgements:

I would like to thank the Laboratory of Endocrine and Metabolic Research and all my colleagues for their precious help in writing this thesis.

I would like to thank my supervisor and co-supervisor Professor Laura Fugazzola and PhD. Dr. Marina Muzza for the opportunity to learn how to be a better researcher in the field of thyroid cancer and for proofreading this work.

I would like to thank my family for providing me with financial as well as psychological support during these three difficult years.

I would like to thank my friends Luca Bellavia and Andrea Moi and my girlfriend Chiara Poletti for their patience and sustained support whenever I wasn't feeling myself.

Finally, I would like to thank PhD Coordinator Professor Chiarella Sforza and the Doctoral Programme of Translational Medicine for their efforts in teaching the importance of aiming research towards a better understanding of pathology in favour of diagnostic and therapeutic applications.